# Thesis

# Diagnostic and prognostic value of amyloid scintigraphy in patients with suspected cardiac amyloidosis: a retrospective study

submitted by

**Mina Ashjaei**

in partial fulfillment of the requirements for the degree of

**Doktorin der gesamten Heilkunde**

**(Dr.in med. univ.)**

at the

**Medical University of Graz**

executed at the

**Department of Radiology**

Division of Nuclear Medicine

under the supervision of

**Univ. FÄ Dr.in Susanne Stanzel**

**Univ. Prof.in Dr.in Reingard Maria Aigner**

Graz, am 08.02.2024

## *Statutory Declaration*

*I hereby declare that I have authored this diploma thesis fully on my own, that I have not used any other than the declared sources, and that I have explicitly marked all material which has been quoted either literally or by content from the used sources.*

*Graz, 08.02.2024* *Mina Ashjaei eh*

## *Acknowledgement*

*I would like to acknowledge and give my warmest thanks to my supervisors, Univ. FÄ Dr.in Susanne Stanzel and Univ. Prof.in Dr.in Reingard Maria Aigner, who made this work possible.*

*Lastly, I am extremely grateful to my lovely mother, Anni, my role model, father Dr. Kazem Ashjaei, and my little brother for their love and prayers. Their belief in me has kept my spirits and motivation high during these years. I also want to express my thanks to my grandmother and her valuable prayers. RIP, Grandma.*

## *Contents*

## Abbreviations

| | |
|---|---|
| AA | amyloid amyloidosis |
| AL | amyloid light chain |
| AG-10 | Acoramidis-10 |
| ATTR | amyloid-transthyretin |
| ATTRm | hereditary transthyretin amyloidosis (mutation) |
| ATTRwt | wild-type transthyretin amyloidosis |
| ATTRv | transthyretin amyloidosis variant |
| ANOVA | analysis of variance |
| AUC | Area under the curve |
| CA | cardiac amyloidosis |
| CMR | cardiac magnetic resonance |
| CT | computer tomography |
| $^{11}$C-PiB | C-11-labeled Pittsburgh Compound-B |
| 2D | 2-dimensional |
| DNA | deoxyribonucleic acid |
| ECG | electrocardiogram |
| ECV | extra-cellular volume |
| FAP | familial amyloid polyneuropathy |
| FLC | Free light chain immunoglobulins |
| FDA | Food and Drug Administration |
| H/CL | heart-to-contralateral lung ratio |
| HFpEF | heart failure with preserved ejection fraction |
| $^{111}$In-antimyosin | Indium-111-monoclonal antimyosin |
| $^{123}$I-MIBG | 123I-meta-iodobenzylguanidine |

| | |
|---|---|
| k | Kappa |
| λ | lambda |
| LV | left ventricle |
| LGE | late gadolinium enhancement |
| Mbq | megabecquerel |
| min | minute |
| MRI | Magnetic resonance imaging |
| MRT | Magnetresonanztomographie |
| mo | months |
| NSAID | nonsteroidal anti-inflammatory drug |
| NT-proBNP | N-terminal pro brain natriuretic peptide |
| OLT | Orthotopic liver transplantation |
| Pts | Patients |
| PET | positron emission tomography |
| p.i. | post injection |
| RV | right ventricle |
| SAA | serum amyloid A |
| SCD | sudden cardiac death |
| SPECT | single photon emission computed tomography |
| $^{99m}$Tc-aprotinin | Technetium-99m-labelled aprotinin |
| $^{99m}$Tc-DPD | Technetium-99m-labelled 3,3-diphosphono-1,2-propanodicarboxylic acid |
| $^{99m}$Tc-PYP | Technetium-99m-labelled pyrophosphate |
| $^{99m}$Tc-PYP | Technetium-99m-labelled pyrophosphate |
| TnT | Troponin T |
| TTR | Transthyretin |

## List of Figure

# List of Tables

## Zusammenfassung

**Einleitung:** Systemische Amyloidose umfasst eine Gruppe von Erkrankungen, die durch die extrazelluläre Ansammlung unlöslicher fibrillärer Proteine gekennzeichnet sind, was zu Strukturstörungen in den betroffenen Geweben und einer Beeinträchtigung der Organfunktion führt. Von besonderem Interesse ist die kardiale Form der Amyloidose. Das klinische Erscheinungsbild von Amyloidose-Patienten variiert je nach Art der Herzbeteiligung. Während die Echokardiographie als Goldstandard für die nicht-invasive Diagnose einer Amyloid- Kardiomyopathie gilt, erfordert die endgültige Diagnose einer Amyloidose typischerweise die Biopsie des betroffenen Organs. In jüngster Zeit hat sich die Amyloid-Szintigraphie mit $^{99m}$Tc-Pyrophosphat (PYP) als wertvolles klinisches Instrument für die kardiale Bildgebung bei Amyloidose herausgestellt.

**Ziel:** Ziel dieser Studie ist, sowohl den diagnostischen Stellenwert als auch die prognostische Wertigkeit der Amyloid-Szintigraphie unter Verwendung von $^{99m}$Tc-Pyrophosphat bei Verdacht auf kardiale Amyloidose zu bewerten.

**Methoden und Materialien:** Es wurde eine retrospektive Analyse an 150 Personen durchgeführt, bei denen der Verdacht auf kardiale Amyloidose bestand. Zwischen Juli 2018 und Juni 2022 wurde mittels einer Amyloid-Szintigraphie mit $^{99m}$Tc-Pyrophosphat untersucht. Die Ergebnisse der Amyloid-Szintigraphie (Perugini-Score 0-3, Herz/kontralaterale Lungen Ratio (H/CL-Ratio)) wurden mit den Ergebnissen einer Myokardbiopsie und/oder einer Herz-MRT verglichen. Die Patient*innen wurden in die verschiedenen Gruppen des Perugini-Scores (0, 1, 2, 3) und der H/CL Ratio (größer oder kleiner 1,5) eingeteilt. Die mediane Nachbeobachtungszeit betrug 9 Monate. Darüber hinaus wurde der Zusammenhang zwischen dem Perugini-Score und der Lebenserwartung mittels Log-Rank-Test untersucht.

**Ergebnisse:** Es wurde bei 16 Patient*innen eine Myokardbiopsie und bei 77 Patient*innen eine Herz-MRT durchgeführt. Die Amyloidszintigraphie mit $^{99m}$Tc-PYP wurde bei 133 Patient*innen (88,7%) positiv gewertet basierend auf die visuelle Beurteilung des myokardialen Tracer-Uptakes in der planaren Szintigraphie (Perugini-Score 1-3). Im Gegensatz dazu wurde die Amyloidszintigraphie bei 17 Patient*innen (11,3%) negativ gewertet (Perugini-Score 0). In der semiquantitativen Beurteilung

hatten 80 Patient'*innen (53,3%) eine H/CL-Ratio > 1,5 und 70 Patient*innen (46,7%) eine H/CL Ratio ≤ 1,5. Bei Verwendung der Myokardbiopsie als Goldstandard ergab sich für den Perugini-Score eine Sensitivität von 92% und eine Spezifität von 33% und bei Verwendung der Herz-MRT als Goldstandard 91% bzw. 15%. Im Gegensatz dazu zeigte die quantitative H/CL-Ratio eine Spezifität von 67 % und eine Sensitivität 54% bei Verwendung der Myokardbiopsie als Goldstandard und 64% bzw. 64% bei Verwendung der Herz-MRT als Goldstandard.

Hinsichtlich der prognostischen Wertigkeit der Amyloidszintigraphie mit $^{99m}$Tc-PYP zeigte sich kein signifikanter Unterschied im Überleben zwischen Patient*innen mit Perugini-Score 1-3 und Patient*innen mit Perugini-Score 0 sowie Patient*innen mit H/CL Ratio >1,5 und ≤1,5.

**Schlussfolgerung:** Unsere Studie zeigt eine hohe Sensitivität der $^{99m}$Tc-PYP-Szintigraphie. Sie stellt somit eine nicht-invasive diagnostische Alternativ dar, die herkömmliche diagnostische Methoden wie Myokardbiopsie und Herz-MRT in der Diagnosik und Bewertung von Patient*innen mit kardialer Amyloidose ergänzt. Patient*innen mit Perugini-Score 0 bzw. einer H/CL-Ratio ≤ 1,5 hatten keinen Überlebensvorteil verglichen mit Patient*innen mit Perugini-Score 1-3 bzw. einer H/CL-Ratio > 1,5. Daraus ergibt sich, dass die Stratifizierung nach Perugini-Score und H/CL-Ratio bei Patient*innen mit Verdacht auf kardiale Amyloidose keine prognostische Wertigkeit hat.

**Schlüsselwörter:** Amyloidose, $^{99m}$Tc-PYP-Szintigraphie, H/CL-Ratio

## Abstract

**Introduction:** Systemic amyloidosis encompasses a group of disorders characterized by the extracellular buildup of insoluble fibrillar proteins, leading to structural disturbances in affected tissues and impaired organ function. Of particular interest is cardiac form of amyloidosis. The clinical presentation of amyloidosis patients varies depending on the specific type of cardiac involvement. While echocardiography is regarded as the gold standard for non-invasive diagnosis of amyloidotic cardiomyopathy, a definitive diagnosis of amyloidosis typically necessitates a biopsy of the affected organ. In recent times, amyloid-scintigraphy using $^{99m}$Tc-pyrophosphate (PYP) has emerged as a valuable clinical tool for cardiac imaging in amyloidosis.

**Aim:** The aim of this study is to assess both the diagnostic and prognostic value of amyloid scintigraphy utilizing $^{99m}$Tc-pyrophosphate in suspected cardiac amyloidosis.

**Methods and Materials:** A retrospective analysis was conducted, involving 150 individuals who were suspected of having cardiac amyloidosis. Between July 2018 and June 2022 amyloid scintigraphy with $^{99m}$Tc-pyrophosphate was performed. The results obtained from the amyloid scintigraphy (the Perugini score ranging from 0 to 3, heart-to-lung ratio (H/CL ratio)) were compared with the outcomes of myocardial biopsy and/or cardiac MRI. The patients were categorized into different groups based on the Perugini Score (0, 1, 2, 3) and H/CL ratio (greater or less than 1.5). The median follow-up time was 9 months. Additionally, the association between the Perugini score and life expectancy was examined by the long-rank test.

**Results:** Myocardial biopsies were performed on 16 patients, and 77 patients underwent cardiac MRI. Amyloid scintigraphy with $^{99m}$Tc-PYP was considered positive in 133 patients (88.7%) based on visual assessment on planar images (Perugini score 1-3). By contrast, amyloid scintigraphy was considered negative in 17 patients (11.3%) (Perugini score 0). In the semi-quantitative assessment, 80 patients (53.3%) had a H/CL ratio > 1.5, and 70 patients (46.7%) a H/CL ratio ≤ 1.5. When using myocardial biopsy as the gold standard, the Perugini score showed a sensitivity of 92% and a specificity of 33%, and when using cardiac MRI as the gold standard, 91% and 15%, respectively. In contrast, the quantitative H/CL ratio demonstrated a specificity of 67%

and a sensitivity of 54% using myocardial biopsy as gold standard and 64% and 64%, respectively using cardiac MRI as gold standard.

Regarding the prognostic value of amyloid scintigraphy with $^{99m}$Tc-PYP, no significant differences in survival between patients with Perugini scores 1-3 and patients with Perugini score 0, as well as between patients with H/CL ratio >1.5 and ≤1.5 was found.

**Conclusion:** Our study demonstrates the substantial diagnostic sensitivity of $^{99m}$Tc-PYP scintigraphy, offering a non-invasive diagnostic alternative that complements conventional diagnostic methods like myocardial biopsy and cardiac MRI in the evaluation of patients with cardiac amyloidosis. Patients with Perugini score 0 and a H/CL ratio ≤ 1.5, respectively had no survival benefit compared to patients with Perugini score 1-3 and a H/CL ratio > 1.5, respectively. This shows that stratification according to Perugini score and H/CL ratio has no prognostic value in patients with suspected cardiac amyloidosis.

**Keywords:** amyloidosis, $^{99m}$Tc-PYP scintigraphy, H/CL ratio

# 1 Introduction

## 1.1 Amyloidosis

Amyloidosis is a group of diseases caused by the accumulation of insoluble proteins [1], leading to organ dysfunction. To date, 25 amyloid-causing proteins that form amyloid fibrils have been classified in humans, with the most common being immunoglobulin light chain (AL) and transthyretin (TTR) [2]. AL amyloidosis fibrils are composed of monoclonal immunoglobulin light chains [3]. Cardiac involvement occurs in 50%–70% of patients with AL amyloidosis and is the predominant clinical feature in patients with nonhereditary ATTR amyloidosis [4].

TTR is produced by the liver and plays a role as a plasma transport protein for thyroxine and vitamin A. ATTR amyloidosis has two main types: hereditary and acquired. Hereditary ATTR amyloidosis results from the misfolding of a mutated form of transthyretin (TTR) and is termed amyloid transthyretin mutant (ATTRm) or variant ATTR (ATTRv). These types of amyloidosis present a wide clinical spectrum, ranging from neurological involvement to cardiac presentation [5]. This heterogeneity is linked to several factors, including specific TTR mutations, patient and transmitting parent gender, geographical distribution, and endemic or non-endemic aggregation [6]. The acquired type is due to the disaggregation of wild-type TTR (ATTRwt), which is also commonly found in the hearts of the elderly (senile TTR amyloid) [7]. The late age of onset is usually after the seventh decade of life, with a strong male predominance (between 25 and 50:1 male-to-female ratio) [8].

Due to the aging population, the ATTRwt variant is projected to become the most frequent form of amyloidosis [7]. While heart amyloidosis is rare, the clinical aspect of heart amyloidosis is mostly the focus.

## 1.2 Cardiac amyloidosis

Cardiac amyloidosis is associated with the deposition of abnormally folded proteins in the extracellular spaces [9], which causes the stiffening of the myocardium and consequently affects the diastolic and systolic functions of the heart.

There are various etiological types of cardiac amyloidosis [10]:

1- Primary amyloidosis (also known as amyloid light chain amyloidosis, or AL amyloidosis) is caused by the deposition of AL fibrils produced by abnormal plasma cells in patients with plasma cell dyscrasias such as multiple myeloma.
2- Secondary amyloidosis (AA amyloidosis) is caused by the deposition of serum amyloid A, which is an inflammatory protein produced in conditions of chronic inflammation.
3- Wild-type transthyretin, or ATTRwt, is caused by age-related amyloid deposition, which is derived from the normal TTR (thyroxine and retinol transport) protein. This is the most common type of cardiac amyloidosis.
4- Familial amyloidosis (ATTRm) is caused by mutant TTR.
5- Isolated atrial amyloidosis is caused by the deposition of amyloid made from the atrial natriuretic peptide.

A simplified schematic in Figure 1 shows the basic transthyretin and cardiac AL amyloidosis [4].

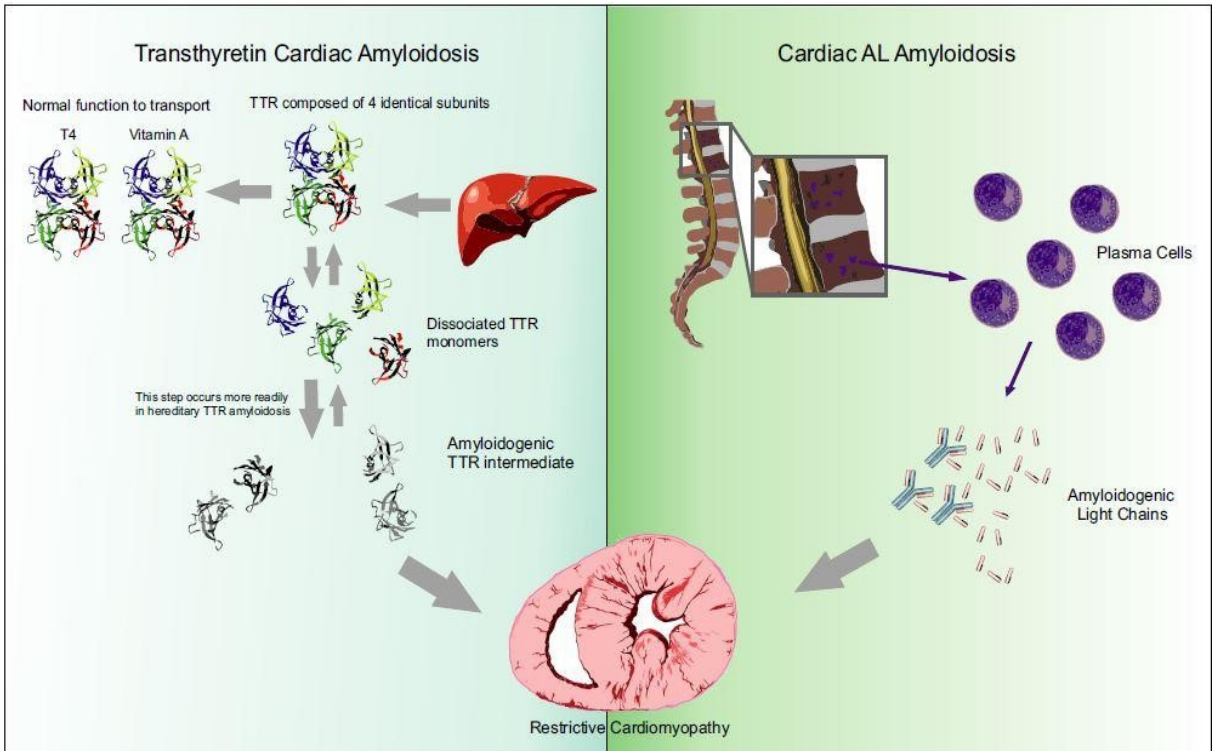


**Figure 1. Overview of cardiac transthyrin (ATTR) and monoclonal immunoglobulin light chain (AL) amyloidosis [4]**

Cardiac AL amyloidosis and transthyretin amyloid (ATTR) amyloidosis are the two common types of cardiac amyloidosis. Cardiac AL amyloidosis is associated with the accumulation of AL amyloidosis fibrils due to B-cell dyscrasia. In ATTR cardiac amyloidosis, the transthyretin (TTR) protein is deposited in tissues, either due to inherited mutations (ATTRm) or the aging process (ATTRwt). As a result, these extracellular amyloid depositions lead to diastolic dysfunction, restrictive cardiomyopathy, and congestive heart failure [11]. Amyloid infiltration in the extracellular matrix significantly alters myocardial stiffness, which is closely associated with the most severe forms of diastolic dysfunction and heart failure, with annual mortality rates ranging from 15% to 50% [12, 13].

### 1.2.1 Epidemiology

Cardiac amyloidosis is a rare disease, with an estimated annual incidence of about 1 per 100,000, or approximately 2500-5000 new cases each year for AL amyloidosis. Recent research indicates that ATTRwt (wild-type transthyretin) might be responsible for up to 10% of cases in elderly patients with heart failure. However, the prevalence of the condition notably rises with advancing age, and histopathological evidence reveals that up to 25% of individuals aged over 80 exhibit demonstrable amyloid deposition [14]. The incidence and prevalence rates of cardiac amyloidosis among hospitalized patients are on the rise, particularly among men. These trends can likely be attributed to a combination of increased awareness and potentially greater utilization of cardiac magnetic resonance imaging in clinical practice [15]. Hereditary transthyretin (ATTRv) amyloidosis is a rare disease. In Sweden the estimated incidence rate was 2 cases per 1 million inhabitants between 2001 and 2008 and has increased from 1.50 cases in 2006-2009 to 4.92 cases per 100,000 persons in 2016-2018 [16].

### 1.2.2 Signs and symptoms

The clinical features of patients with amyloidosis depend on the type of cardiac amyloidosis. The clinical presentation of cardiac amyloid light chain amyloidosis is

multisystemic, involving other organs due to the deposition of amyloid in soft tissues and small vessels. Early detection of cardiac amyloidosis can be challenging through history or initial examination. Common general symptoms include fatigue, palpitations, shortness of breath, abdominal and leg swelling, weight loss, and nocturnal excessive urination. Patients with amyloidosis might also experience other symptoms like paresthesia, carpal tunnel syndrome, autonomic neuropathy with orthostatic hypotension, constipation, and erectile dysfunction.

Wild-type transthyretin amyloidosis predominantly affects the elderly and men, with most patients diagnosed after the age of 70. This group often exhibits significant thickening of the left ventricular wall. Additionally, carpal tunnel syndrome is frequently associated with ATTRwt amyloid deposits. A study revealed that 48% of ATTRwt patients had a documented history of carpal tunnel syndrome, which preceded the onset of clinical heart failure symptoms in 77% of cases. Moreover, the study highlighted that ATTRwt can manifest in diverse tissues beyond the myocardium. For instance, nearly 4% of patients displayed symptoms such as frank hematuria or incidental findings in bladder histology [17].

### 1.2.3 Diagnosis of cardiac amyloidosis

Distinguishing between TTR and AL amyloidosis in diagnosis can be intricate. The diagnostic flowchart for a patient with cardiac amyloidosis is depicted in Figure 2 [18]. Echocardiography serves as the gold standard for the non-invasive diagnosis of amyloidotic cardiomyopathy. Given the potential for misdiagnosis, a biopsy is essential to determine immunohistochemical analysis for a conclusive diagnosis. Free light chain immunoglobulins (FLC) can be detected in the serum or urine of patients with primary amyloidosis. A study demonstrated that the FLC ratio (κ/λ) was abnormal in 88% of patients, which corroborates findings from prior research comparing FLC measurement with electrophoretic tests in serum and urine [19]. Despite these considerations, several methods can be employed to diagnose cardiac amyloidosis, which include:

#### 1.2.3.1 Electrocardiogram

ECG can reveal an increase in the thickness of the left ventricular wall, manifesting as QRS complexes with low voltage, which may raise suspicion of cardiomyopathy. Various electrocardiographic patterns can be present in cardiac amyloidosis (CA). There are significant differences between AL and ATTRwt in terms of ECG findings such as left bundle branch block, low QRS voltage, and total QRS score. Multivariate analysis demonstrated that low QRS voltage remained independently associated with ATTRm pathogenesis, regardless of factors like age, gender, mean LV wall thickness, and pericardial effusion. Additionally, left bundle branch block was observed in 40% of ATTRwt patients [20]. The most typical pattern is associated with low QRS voltages (height <5 mm in all limb leads). In almost 50% of patients with AL-CA, there is a pattern of pseudo infarction associated with poor R-wave progression in the chest leads [7].

#### 1.2.3.2 Transthoracic echocardiography

Transthoracic echocardiography is one of the most common investigations to evaluate the heart in amyloidosis. Cardiac involvement in AL systemic amyloidosis is defined on echocardiography by mainly increased left ventricular (LV) wall thickness and moderate to severe diastolic dysfunction.

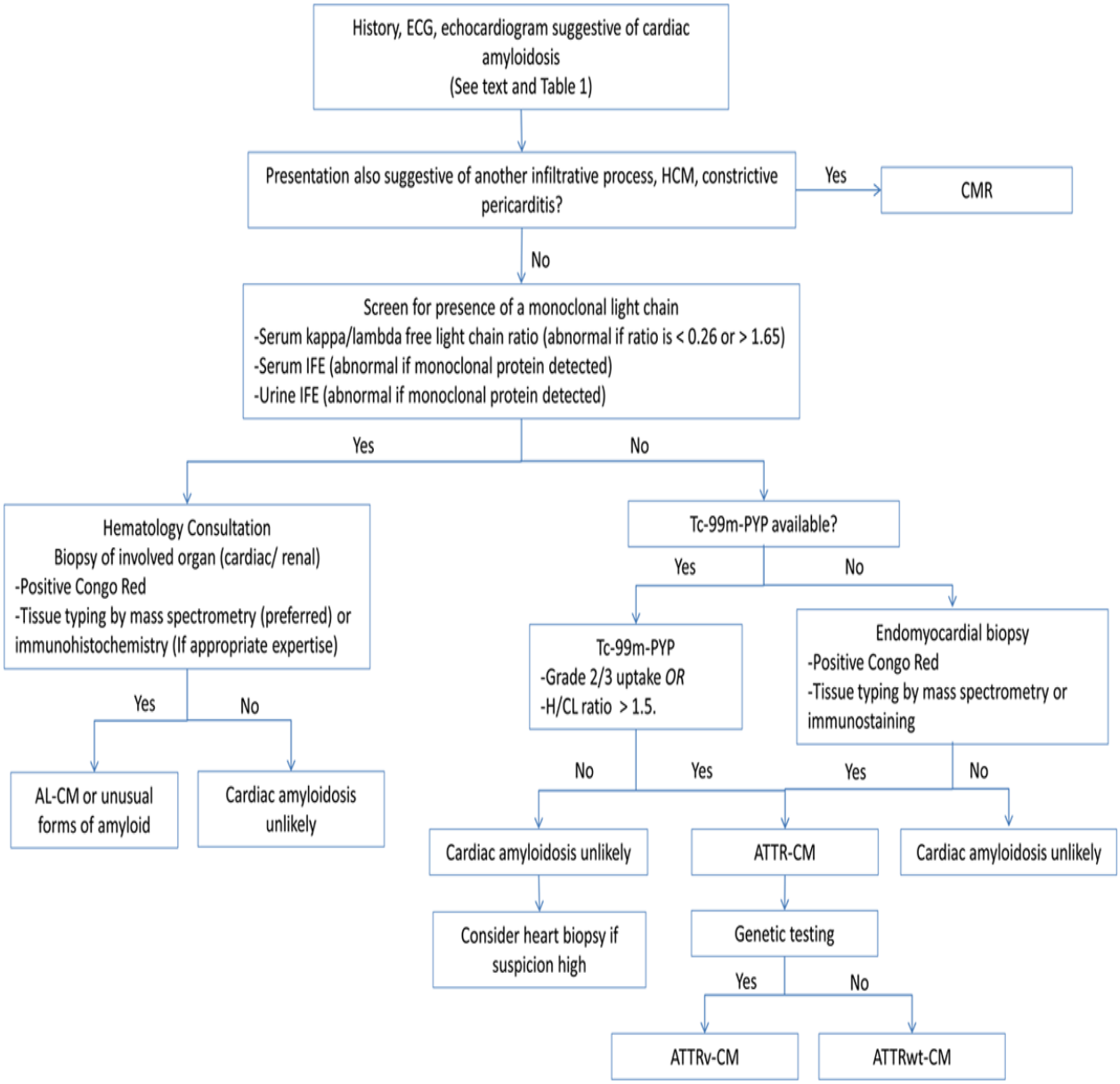


**Figure 2. A typical work-up flowchart for a patient with cardiac amyloidosis [18]**

### 1.2.3.3 Biopsy, histology and immunohistochemistry

The confirmation of amyloidosis diagnosis involves a biopsy of the affected organ. The presence of amyloid deposition is confirmed through histology, utilizing the Congo red method, and immunohistochemical typing employing a panel of monospecific antisera for serum amyloid A (SAA), transthyretin, and kappa and lambda light chain proteins.

#### 1.2.3.4 Imaging

Imaging techniques such as radionuclide scanning, and cardiovascular magnetic resonance (CMR) have proven to be valuable clinical tools in amyloidosis.

##### *1.2.3.4.1 CMR*

The ratio of cell volume to extracellular volume (ECV) is a characteristic of normal organs and tissues, which can alter in diseases due to factors like cell hypertrophy, hyperplasia, loss, or extracellular expansion [21]. This expansion may involve increased water content, diffuse fibrosis, or the accumulation of pathological substances like amyloid. CMR offers more precise measurements of left ventricular (LV) volume, mass, and wall thickness compared to echocardiography, making it highly beneficial for disease evaluation. CMR is highly beneficial when differentiating amyloidosis from other causes of LV thickening, such as hypertension, where routine echocardiography might fall short [7]. A recent development, the equilibrium contrast CMR technique, has unveiled considerably larger extracellular myocardial volume in cardiac amyloidosis than in other conditions [7].

##### *1.2.3.4.2 Radionuclide imaging*

*1.2.3.4.2.1 $^{99m}$Tc-pyrophosphate, $^{99m}$Tc-DPD*

Radiolabelled phosphate derivatives, initially developed as tracers for bone scan, such as $^{99m}$Tc-DPD ($^{99m}$Tc-3,3-diphosphono-1,2-propanodicarboxylic acid) can be harnessed to identify amyloid in the heart [22]. Several $^{99m}$Tc-labelled phosphate derivatives, including $^{99m}$Tc-PYP ($^{99m}$Tc-pyrophosphate) and $^{99m}$Tc-DPD, have all demonstrated effective detection of transthyretin cardiac amyloid [22-24]. Among these bone-seeking tracers, $^{99m}$Tc-DPD has been extensively employed in the field as a tracer for diagnosing transthyretin cardiac amyloidosis and is even capable of detecting the disease in its early stages [25]. Imaging with $^{99m}$Tc-DPD has displayed a sensitivity of 100% and specificity of 88% in detecting transthyretin cardiac amyloid, in addition to a high negative predictive value (100%) for excluding cardiac amyloid

light chain involvement [26]. It also boasts a positive predictive value of 88% for diagnosing transthyretin cardiac amyloid [26].

Bokhari S et al. have demonstrated that $^{99m}$Tc-PYP amyloid scintigraphy can effectively differentiate between AL and ATTR cardiac amyloidosis in patients previously diagnosed with AL and ATTR through biopsy [23]. This method holds promise as a straightforward and widely accessible approach to identifying individuals with ATTR cardiac amyloidosis.

Figure 3 presents a consensus algorithm for the non-invasive diagnosis of cardiac amyloidosis through bone scintigraphy [27]. This method holds promise as a widely accessible approach to identifying individuals with ATTR cardiac amyloidosis.

It's worth highlighting that radionuclide imaging can play a pivotal role in the non-invasive diagnosis of cardiac involvement. Within radionuclide imaging, the assessment of myocardial uptake of diphosphonate radiotracers, such as $^{99m}$Tc-PYP and $^{99m}$Tc-DPD, offers significant sensitivity in detecting both ATTR-CA and AL-CA.

Notably, myocardial uptake is almost absent in most cases of AL-CA, marking a crucial distinction from ATTR-CA, which exhibits a strong affinity for bone tracers.

Furthermore, the utilization of $^{99m}$Tc-DPD SPECT-CT has demonstrated high sensitivity in detecting cardiac amyloidosis [7].

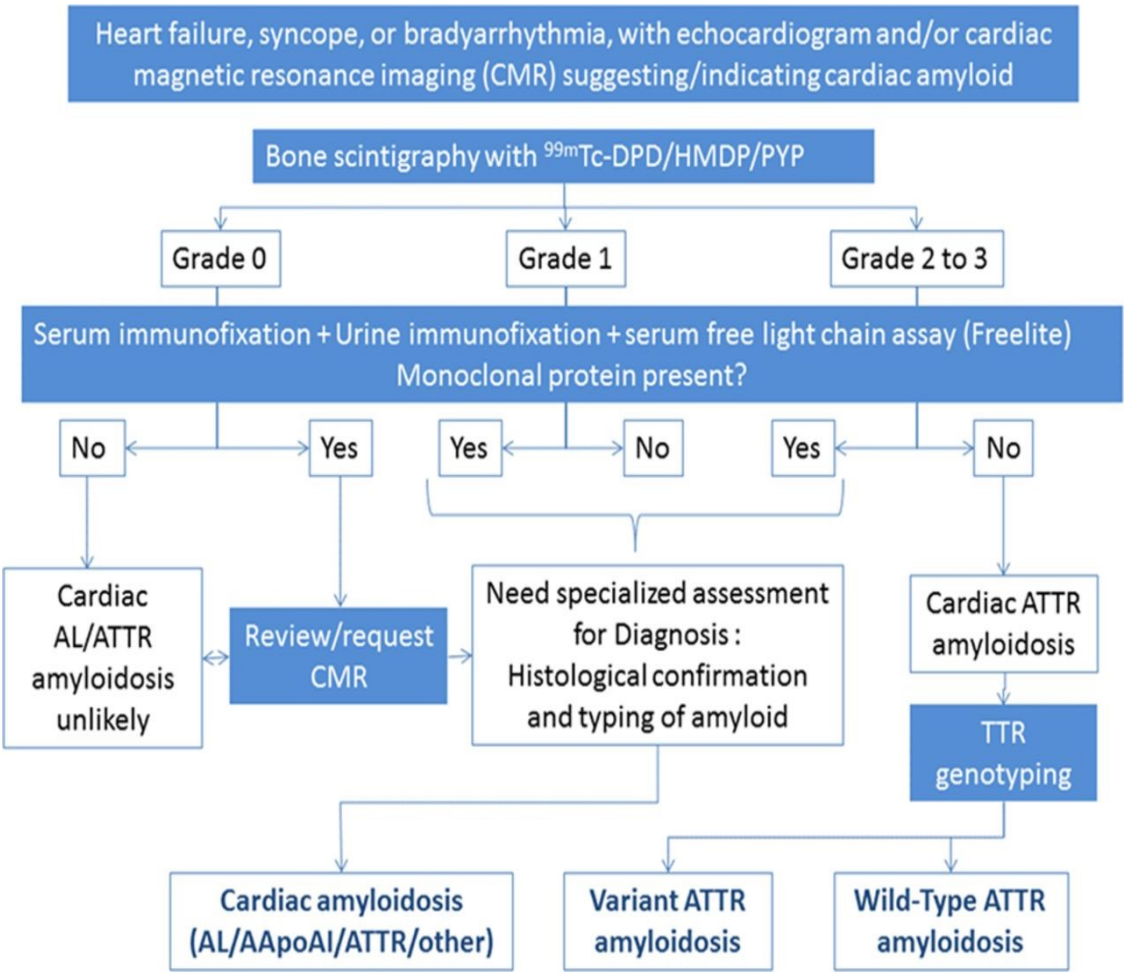


**Figure 3. A consensus algorithm for the non-invasive diagnosis through bone scintigraphy in cardiac amyloidosis patients [27]**

Figure 4 below presents representative examples that illustrate the spectrum of cardiac scintigraphy using $^{99m}$Tc-PYP in ATTR cardiac amyloidosis [28]. The top row of images (a) showcases $^{99m}$Tc-PYP whole-body planar images, while the middle row of images (b) displays $^{99m}$Tc-PYP cardiac SPECT images acquired at 2.5 hours post-injection. The bottom row of images (c) exhibits cardiac magnetic resonance late gadolinium enhancement images (CMR) in the 4-chamber view.

In these images, the control patient exhibits no detectable $^{99m}$Tc-PYP myocardial uptake in both planar and SPECT imaging (grade 0), and no evidence of late gadolinium enhancement (LGE) can be observed in the magnetic resonance imaging. For the patient with AL amyloidosis, grade 1 uptake (myocardial uptake less than rib uptake) is seen, and CMR demonstrates concentric left ventricular thickening along with diffuse LGE characterized by subendocardial predominance. In the third column,

the patient with ATTR cardiac amyloidosis presents grade 2 uptake (myocardial uptake equal to rib uptake), while CMR reveals bi-atrial dilation, diffuse left ventricular thickening, and LGE. Finally, the patient with ATTR cardiac amyloidosis in the fourth column displays grade 3 uptake (myocardial uptake greater than rib uptake, accompanied by soft tissue uptake attenuation), and CMR displays diffuse LGE.

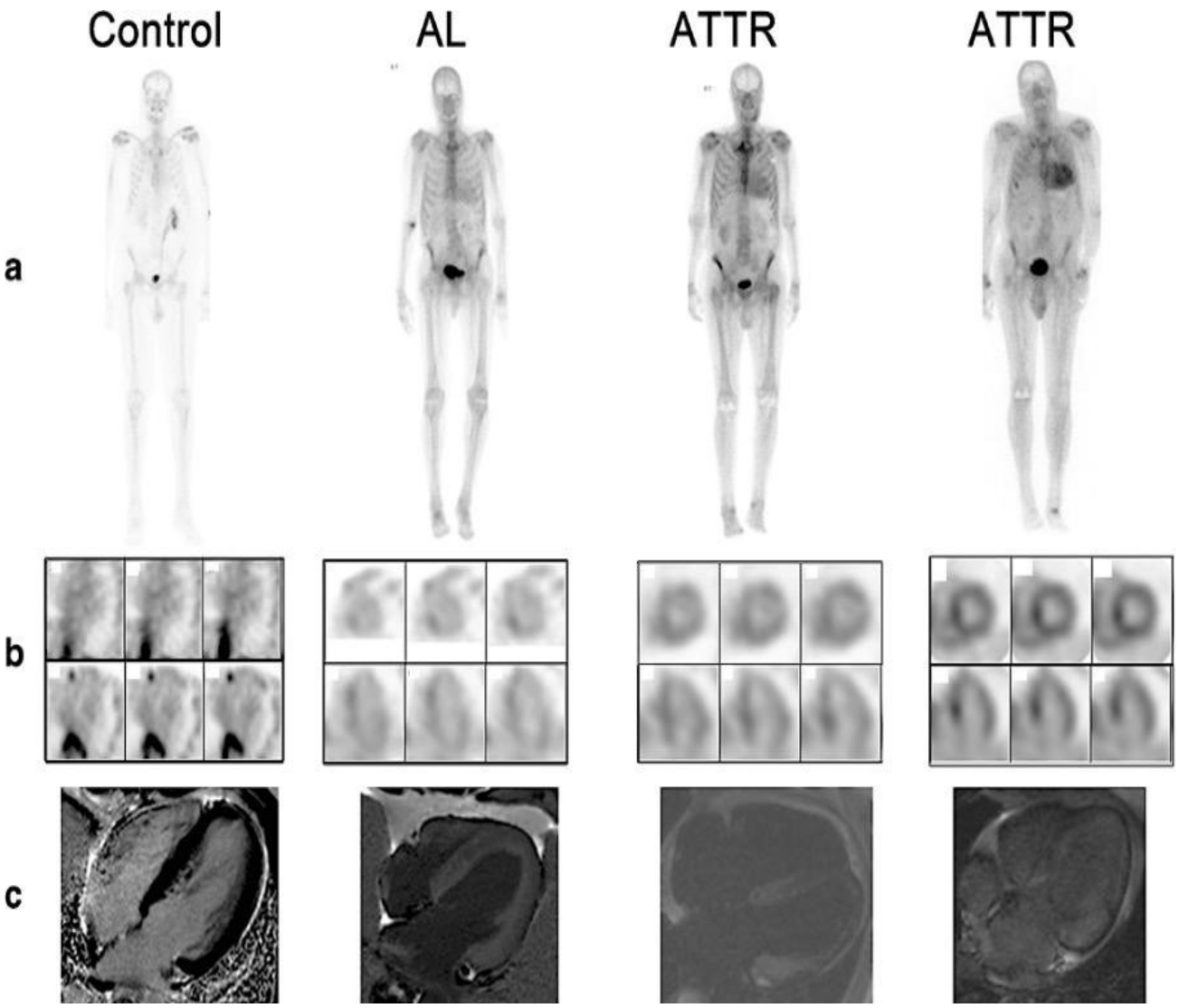


**Figure 4. Respresentative examples of amyloid scintigraphy with $^{99m}$Tc-PYP in ATTR cardiac amyloidosis [28]**

Several other tracers can also be employed in the diagnosis of cardiac amyloidosis:

**$^{99m}$Tc-aprotinin:** Scintigraphy with $^{99m}$Tc-aprotinin has demonstrated notable sensitivity and specificity as a diagnostic tool in patients suspected of having

amyloidosis. This noninvasive technique minimizes patient stress and is effective in detecting a wide array of lesions [29].

**$^{111}$In-antimyosin:** Originally developed for detecting acute myocardial infarction, $^{111}$Indium-monoclonal antimyosin antibody has found utility in diagnosing various cardiovascular diseases where myocyte necrosis is an integral feature [30].

**$^{123}$I-MIBG:** Scintigraphy using $^{123}$I-meta-iodobenzylguanidine (MIBG) enables both qualitative and quantitative assessment of global and regional cardiac sympathetic innervation. It has proven valuable in showcasing cardiac denervation across different pathologies, recently gaining importance in risk stratification for heart failure patients [31].

**$^{11}$C-PiB, $^{18}$F-florbetapir/florbetaben/flutemetamol (PET-tracers for ß-amyloid imaging)**: The utilization of positron emission radiotracers like $^{11}$C-Pittsburgh B compound ($^{11}$C-PiB) or $^{18}$F-florbetaben, coupled with positron emission tomography (PET), has successfully identified cardiac amyloidosis in a noninvasive manner. However, distinguishing between AL and TTR cardiac amyloidosis reliably remains a challenge [32, 33].

### 1.2.4 Treatment of cardiac amyloidosis

The medical management of cardiac amyloidosis is more like the care of heart failure and requires patient education and the cooperation of a team of cardiologists and a nursing team. Weighing daily and regulating fluid intake, limiting sodium and fluids, using diuretics, and blood pressure control are useful. In addition, other methods are used to treat cardiac amyloidosis, including the following:

#### 1.2.4.1 Treatment for ATTR amyloidosis

Current therapeutic strategies for addressing ATTR amyloidosis encompass efforts to reduce wild-type/variant TTR levels and stabilize circulating TTR, aiming to prevent the dissociation of TTR tetramers into monomers, often achieved through liver therapies.

#### *1.2.4.1.1 ATTR stabilization drugs*

Recent developments in the treatment of ATTR cardiac amyloidosis (ATTR-CA) have introduced a range of TTR stabilization drugs. Notably, AG-10, Deflunisal, Epigallocatechin gallate, Tafamidis, and Tolcapone have been employed. Diflunisal, classified as a nonsteroidal anti-inflammatory (NSAID) medication, has displayed TTR stabilization characteristics in vitro. However, its evaluation has primarily occurred through small, nonrandomized, and mostly noncomparative single-arm prospective cohort trials, predominantly focusing on ATTRv-CA [34].

Tafamadis, an analog of diflunisal, similarly exhibits TTR stabilization characteristics without being classified as an NSAID. Worth mentioning, tafamidis stands out as the sole treatment approved by the US Food and Drug Administration (FDA) for both forms of ATTR-CA [35].

A significant study, the multinational ATTR-ACT trial, encompassed patients with cardiomyopathy (comprising 24% ATTRv and 76% ATTRwt) who were randomly assigned to receive either tafamidis 80 mg, tafamidis 20 mg, or a placebo once daily for a period of 30 months. This study revealed that tafamidis resulted in notably reduced all-cause mortality (42.9% vs. 29.5%) as well as fewer cardiovascular hospitalizations (0.7 per year vs. 0.48 per year) [36].

#### *1.2.4.1.2 Liver transplantation*

Liver transplantation has been practiced since 1990 as a treatment for patients with ATTRv amyloidosis [37]. Orthotopic liver transplantation (OLT) emerged as the pioneering disease-modifying therapy due to the liver's significant contribution to producing unstable circulating TTR. An in-depth analysis focused on the lasting impact of OLT an ATTR reveals that neuropathy and limb dysfunction typically remain irreversible. The 5-year overall survival rate is approximately 100% for ATTRv patients and 59% for non-ATTRv patients [37]. It's notable that neuropathy might manifest as early as 6 years following OLT, and deposits of ATTR may appear even sooner [37].

#### 1.2.4.2 Treatment for AL amyloidosis

Implantable cardiac pacemakers and defibrillators, collectively known as cardiac devices, serve a crucial role in both primary and secondary prevention of sudden cardiac death (SCD) [38]. While heart transplantation remains a viable option, it's worth noting that its feasibility is often limited among elderly patients with cardiac amyloidosis. However, heart transplant outcomes have shown promise in younger patients. Following heart transplantation, a course of chemotherapy becomes imperative to suppress plasma cell dyscrasia and prevent the recurrence of cardiac amyloidosis [39]. For AL amyloidosis treatment, the cornerstone lies in proteasome inhibitor-based chemotherapy, frequently incorporating daratumumab. Additionally, when feasible, autologous stem cell transplantation holds significance [35].

### 1.2.5 Prognosis

The severity of cardiac involvement stands as a pivotal determinant in patients' clinical outcomes. To gauge prognosis in amyloidosis, cardiac biomarkers like troponin-T (cTnT) and natriuretic peptides are employed. These biomarkers also offer insight into patients' average life expectancy. In clinical assessments, the widely adopted Mayo staging system, introduced in 2004, is frequently employed [40].

The Mayo staging system categorizes amyloidosis into stages, each corresponding to different biomarker levels and survival periods:

**Stage 1**: Biomarkers below threshold values (TnT), with a median survival of 26.4 months.

**Stage 2**: Biomarkers above threshold values, associated with a median survival of 10.5 months.

**Stage 3**: Both biomarkers above threshold values, leading to a median survival of 3.5 months.

The prognosis varies depending on the type of cardiac amyloidosis. In untreated cases, AL amyloidosis typically leads to a survival time of 9 to 24 months, while ATTR

amyloidosis has a comparatively better prognosis with a survival range of 7 to 10 years. It is important to note that advanced stages of the disease show a 50% one-year survival rate. Studies have shown that patients with cardiac amyloidosis (the majority having ATTR-CA and about 18% having AL) are generally aged between 74 and 90 years [41, 42].

# 2 Methods and materials

For this retrospective study, amyloid scintigraphy examinations conducted between July 2018 and June 2022 were utilized. They were evaluated both qualitatively (using the Perugini score for visual assessment) and quantitatively (by determining the heart/contralateral lung ratio, H/CL). These results were then compared with the findings from potential myocardial biopsies or heart MRI scans. Additionally, the duration of follow-up (including clinical examinations, echocardiographies, and lab tests) was calculated in months from the time of amyloid scintigraphy until either death or November 2022. The predictive significance of amyloid scintigraphy was assessed by correlating the Perugini score and the H/CL ratio with the predicted lifespan in months.

## 2.1 Study population

This retrospective study includes 150 patients (42 females and 108 males) with suspected cardiac amyloidosis. The patients underwent an amyloid scan with $^{99m}$Tc-PYP between 2018 and 2022 at the Division of Nuclear Medicine in Graz. Patient information was gathered from the open MEDOCS database. During evaluation, data were made anonymous by assigning them consecutive codes. Unencrypted patient information was accessible only to two individuals: the graduate student and the supervisor. Patients were followed up for a median duration of 9 months.

Inclusion criteria encompassed patients with suspected cardiac amyloidosis, notably those with cardiomyopathy. Exclusion criteria involved pregnancy and breastfeeding.

The examined patients ranged in age from 14 to 90 years, with a mean age of 71 ±11.4 years. The mean age for males was 70.6 ±11.7 years, while for females it was 73.5 ±10.2 years. The proportion of male patients was significantly higher than that of female patients, indicating an imbalance in gender distribution.

The primary focus of the analysis involved categorizing patients based on Perugini scores of 0, 1, 2, or 3. Secondary objectives included evaluating the heart/contralateral lung (H/CL) ratio and determining the number of months for follow-up until death or

November 2022. Additionally, the outcomes of patients who underwent myocardial biopsy or cardiac MRI were compared to the results of the amyloid scan.

## 2.2 Tracer principle

A tracer is a molecule that participates in specific metabolic processes within an organism [43]. It distinguishes itself from natural metabolites due to its radiolabelled properties, allowing its distribution to be monitored externally. Consequently, radioactive tracers are utilized to visualize the metabolism of organs in nuclear medicine imaging. A scintigraphic tracer typically comprises two main components:

- A molecule (drug) that exhibits specific binding to a molecular target or is metabolized by it (e.g., receptor, enzyme). This leads to the distribution of the tracer.
- A radioactive isotope (label, tag, marker) that enables the detection of the molecule. This allows the utilization of techniques such as SPECT or PET for imaging.

The development of a molecular imaging technique begins with identifying appropriate molecular targets that are specific to a particular disease process.

These targets differ primarily due to various barriers that typically need to be overcome following intravenous injection. For instance, intracellular targets face the challenge of crossing the cell membrane, while brain targets encounter the blood-brain barrier. The accessibility of a target in vivo depends primarily on the selected target-affine structures (such as antagonists, agonists, enzyme inhibitors, etc.). Successful molecular imaging also hinges on having suitable affinity and the lowest possible metabolism of the modified or labeled basic structure [43].

Figure 5 illustrates the radioactive labelling principle schematically. The radioactive isotope is bound to the carrier molecule via a linker, which acts a connecting piece. The carrier molecule establishes contact with the target organ by selectively binding to a molecular target (such as a receptor or enzyme).

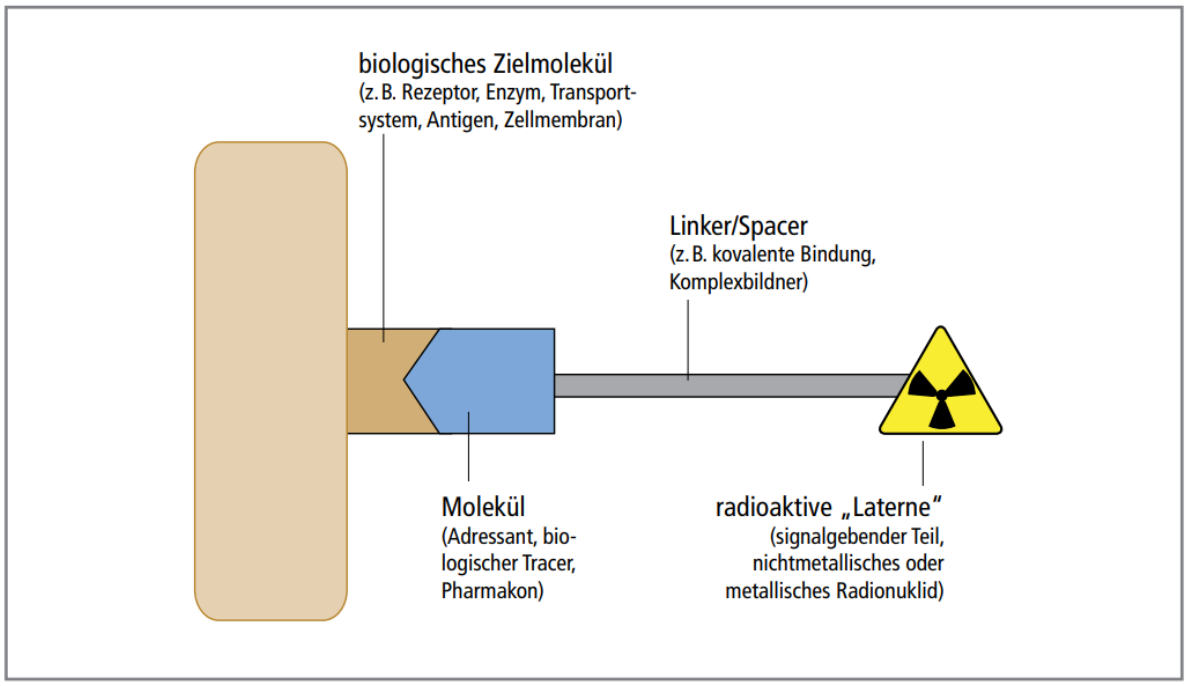


**Figure 5. The detection principle and structure of a radiotracer [43]**

## 2.3 Gamma camera

A gamma camera detects and visualizes the spatial distribution of gamma radiation sources. It was formerly called the Anger camera after its inventor Hal Anger. Stationary gamma cameras that do not move during acquisition (planar scintigraphy) can be distinguished from moving cameras that move in a plane along the longitudinal axis of the patient (whole-body scintigraphy) and those that rotate around the patient (SPECT). Photons strike almost perpendicularly the NaI(Tl) crystal through the lead collimator and produce light proportional to their energy. Then the photomultiplier converts the light signal into an electric signal. Electronics calculate the location of entry using the relative light yield of the photomultiplier (PM) and energy of the photon via the absolute light yield (Figure 6) [43].

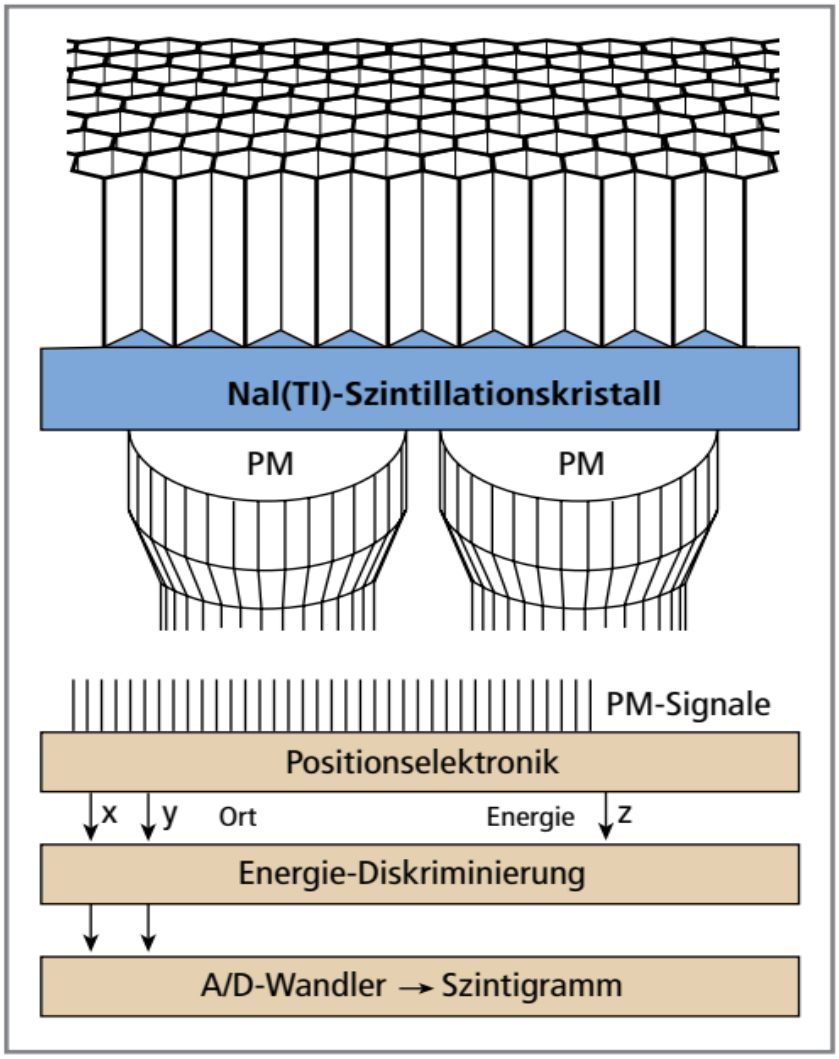


**Figure 6. Schematic diagram showing the major components of a gamma camera [43]**

Resolution and homogeneity are key quality parameters for a gamma camera. Resolution is primarily determined by the collimator [43]. Different types of collimators are named based on their properties, ranging from UHR (ultra-high resolution, high resolution with low sensitivity) to AP (all-purpose, medium resolution and sensitivity) to HS (high sensitivity, high sensitivity with low resolution).

The detector, combining crystal, PM arrangement, and electronics, typically resides in a common casing, the camera head. Modern cameras have 2 or 3 heads because this allows twice as many events to be registered for the same measurement time, or the examination time to be halved for the same number of events [43].

## 2.4 Single-photon emission computed tomography (SPECT)

Planar scintigraphy's drawback lies in its representation of sequential decay events within the patient: they manifest in the same location on the scintigram, thus conveying two-dimensional information without depth details [43]. To ascertain the three-dimensional radionuclide distribution, a tomographic method is essential. This approach, known as "slice imaging," employs radionuclides like $^{99m}$Tc, leading to single photon emission computed tomography (SPECT).

SPECT entails rotating gamma camera detector heads around the patient's longitudinal axis, capturing planar scintigrams from varying angles. Each scintigram projects the three-dimensional nuclide distribution into a two-dimensional form. Reconstruction of the nuclide distribution is the aim. With this, it is assumed that the nuclide distribution in a layer perpendicular to the rotation axis (transaxial or transversal layer) can be calculated entirely from the corresponding lines of the individual planar scintigrams.

Filtered backprojection (FBP) is a computational method for tomographic reconstruction. It projects content from all angles back to the object plane and filters to remove overlap, resulting in transaxial sections approximating 3D radionuclide distribution. FBP doesn't fully address physical realities like limited resolution and gamma radiation attenuation in the patient, so iterative methods are used for accuracy. Modern SPECT systems use semiconductor detectors like Cadmium Zinc Telluride (CdZnTe), acquiring projections from various angles for overlap-free images. SPECT provides comparability with CT, MRI, Positron Emission Tomography (PET), but can't capture rapid metabolic processes because more than 30 minutes elapse between the first and last acquisition angle. SPECT/CT combines dual-head gamma cameras and CT scanners [43].

## 2.5 Scintigraphic examinations

A scintigram, named after "scintilla" meaning "spark" in Latin, visualizes activity distribution for a specific body function at a moment (static scintigram). It's a straightforward method to show functional processes. Areas with heightened activity

reveal hyperactive function. Conversely, heightened activity accumulation in a focus suggests functional overactivity. The differentiation between functionally active and inactive tissue often impacts clinical decisions. These processes are usually based on molecular functional processes, which is why scintigraphic imaging is also referred to as molecular imaging. This functional information cannot usually be obtained by imaging techniques such as ultrasound, X-ray diagnostics, computed tomography (CT) or magnetic resonance imaging (MRI), which have better spatial resolution but only depict morphology [43].

## 2.6 Technetium-99m ($^{99m}$Tc)

The radionuclide most commonly used to date for conventional planar scintigraphy and SPECT is technetium-99m ($^{99m}$Tc), which was recognized for diagnostic nuclear medicine as early as 1960. The exceptional significance of the radionuclide $^{99m}$Tc in in-vivo nuclear medicine diagnostics is attributed to the following properties: Its half-life (T1/2) of 6.02 hours allows convenient examination of physiological processes, while maintaining a low and acceptable radiation dose for patients. With a gamma line at 141 keV, $^{99m}$Tc falls within the optimal resolution range of 100 to 200 keV for gamma cameras equipped with conventional NaI(Tl) detector heads. $^{99m}$Tc has gained prominence and widespread use in nuclear medicine due to its easy accessibility through commercially available $^{99Mo}$ / $^{99m}$Tc mother-daughter nuclide generators [43].

## 2.7 $^{99m}$Tc-PYP scintigraphy

$^{99m}$Tc-PYP scanning combined with Single-Photon Emission Computed Tomography (SPECT) is a common approach in cardiac imaging for diagnosing amyloidosis.

The procedure begins with the injection of $^{99m}$Tc-PYP into a peripheral vein. Following the injection and its circulation in the bloodstream, the tracer accumulates in the bones and, in cases of cardiac amyloidosis, also in the myocardium. Subsequently, planar imaging and optionally SPECT are conducted after a certain period of time.

In this study, all patients received intravenous injections of 534–730 MBq of $^{99m}$Tc-PYP (mean [SD]: 534.46 [44.77], min: 324, max: 730 MBq). A static planar image of the thorax was taken 60 minutes post-injection. Dynamic thorax imaging (0-60 min post-injection) was conducted in 70 patients, while whole-body images were acquired in 134 patients 3-4 hours and 30 minutes post-injection. Additionally, 48 patients underwent SPECT/CT imaging of the heart.

### 2.8 Perugini scoring system

In order to interpret $^{99m}$Tc-PYP planar images, we used the visual grading rule reported by Perugini et al. [26] which consisted of:

Grade 0: no cardiac uptake

Grade 1: mild cardiac uptake visible but less than skeletal uptake

Grade 2: visible moderate cardiac uptake equal to or greater than skeletal uptake

Grade 3: strong cardiac uptake with little or no skeletal uptake.

In the following figures, there are examples of patients' images of $^{99m}$Tc-PYP amyloid scintigraphy according to the Perugini score classification.

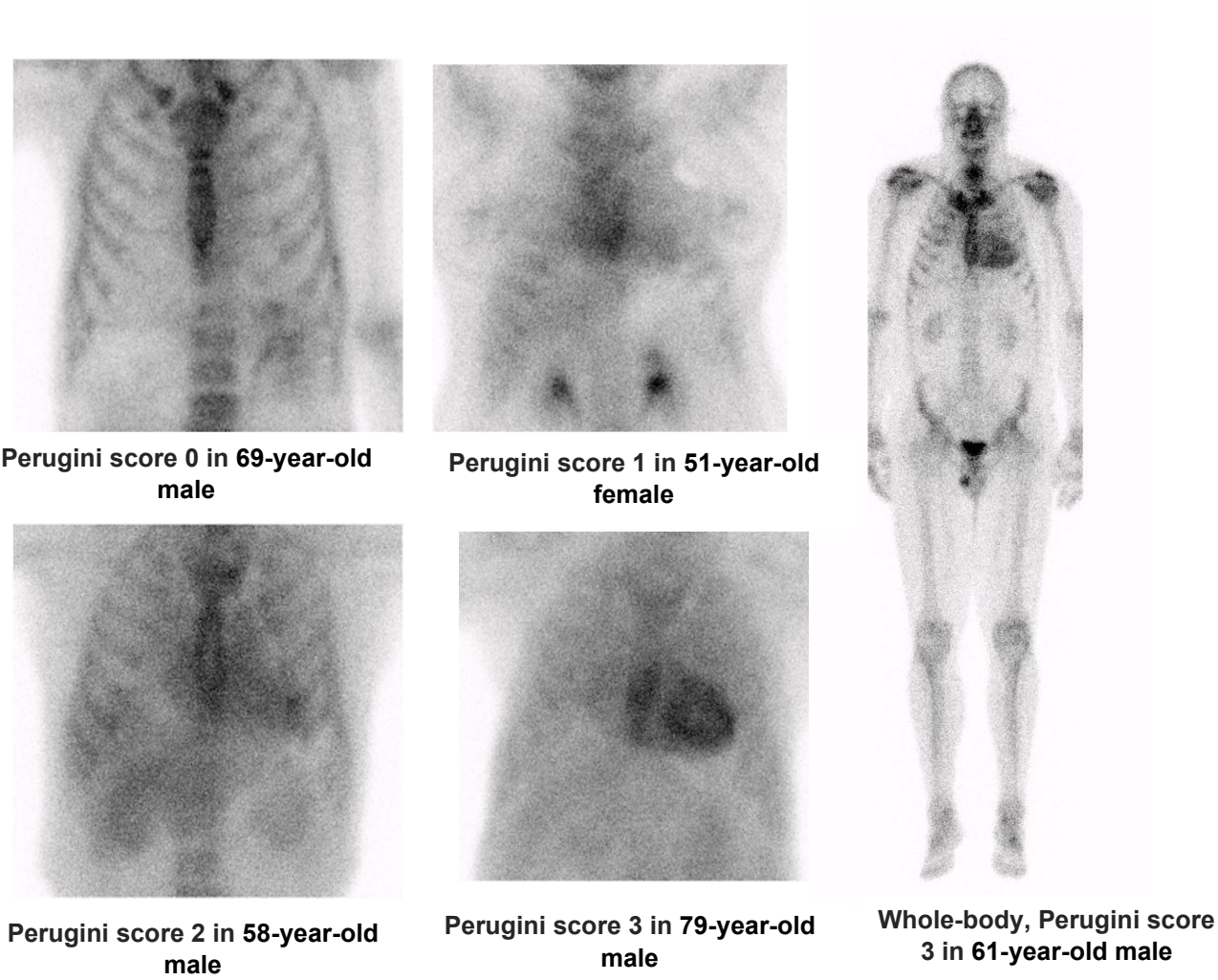


**Figure 7. Images of amyloid scintigraphy with $^{99m}$Tc-PYP based on Perugini scoring system**

### 2.9 Heart-to-contralateral lung (H/CL) ratio

Longitudinal regions of interest (ROI) were delineated over the heart on the planar images and mirrored across the contralateral chest to compensate for background and rib interference. Subsequently, a heart-to-contralateral lung (H/CL) ratio was computed by dividing the mean counts of the heart ROI by the mean counts of the contralateral chest ROI. According to the literature, H/CL ratios ≥1.5 at one hour were categorized as ATTR positive, while ratios <1.5 were labeled as ATTR negative [44].

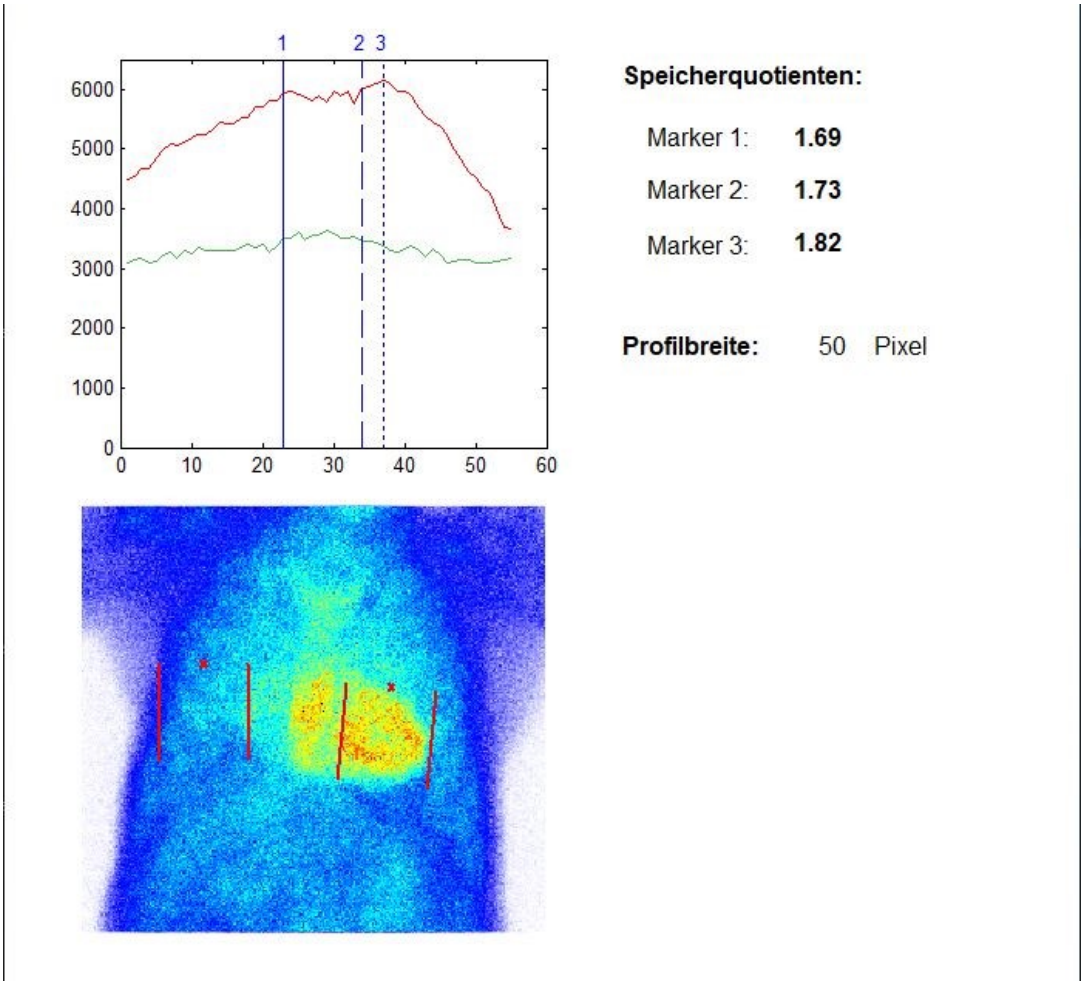


**Figure 8. H/CL ratio in case of a 79-year-old male with visible $^{99m}$Tc-PYP myocardial uptake in planar images**

## 2.10 Cardiac biopsy

While heart biopsy is considered a definitive method for diagnosing amyloidosis, it demands a high level of technical expertise due to potential complications and inherent risks [45]. The diagnostic process involves immunohistochemical staining of biopsied samples. To avoid false negative results, specific antiserum/antibodies targeting different potential types of amyloid are initially tested on myocardial tissue. The accuracy of staining results heavily depends on factors like tissue processing, effective antigen clearance, and antibody quality, particularly in formalin and paraffin-embedded (FFPE)-fixed biopsies. In AL amyloidosis, the lambda light chains are the predominant amyloidogenic precursors, necessitating specific staining for positive

identification. In ATTR CA cases, immunostaining for TTR must be highly positive and consistent with Congo red-positive amyloid deposits [46].

### 2.11 Cardiac MRI

Cardiac MRI serves as a valuable tool for evaluating cardiac structure and function while aiding in the characterization of myocardial tissue [47]. Recognized for its high sensitivity and specificity, cardiac MRI is a diagnostic modality highly suited for assessing both AL and ATTR cardiac involvement [48]. Interpretation of cardiac MRI findings should consider the clinical context alongside other test results [47]. Cine cardiac MRI and late gadolinium enhancement (LGE) MRI are typically employed for imaging in cardiac amyloidosis (CA) [47]. This approach involves assessing left ventricular (LV) thickening, often of a concentric and symmetrical nature [47]. While LV thickening is more prevalent in ATTR patients compared to AL patients, the distribution of distinct morphological phenotypes remains consistent between ATTRm and ATTRwt patients [47]. In some cases, there's observed involvement of the right ventricle, along with thickening of the atrial wall and the inter-atrial septum.

### 2.12 Ethical approval

The use of patient data in this thesis is based on the submission of necessary documents and the approval of the Ethics Committee of the Medical University of Graz. All conditions for the protection of patient data have been considered.

### 2.13 Statistical analysis

Statistical analysis was conducted using SPSS Statistics 29.0.1.0 (IBM) and GraphPad Prism 6. The data evaluation process employed descriptive statistics. Group comparisons were executed through various methods, including 2-way ANOVA (and nonparametric alternatives), t-test (and nonparametric tests), and the Mann-Whitney test. A significance level of $P<0.05$ was used to define statistical significance.

Sensitivity and specificity are used to measure the probability of a positive result in a diagnostic test for people with the disease and the probability of a negative result for people without the disease, respectively.

# 3 Results

## 3.1 Characteristics of the study population

In this retrospective study, we enrolled 150 patients with suspected cardiac amyloidosis. The characteristics of these individuals are detailed in Table 1. Overall, the patient cohort exhibited an older age profile, with a mean age of 71±11 years. The majority of the participants were male, accounting for 108 out of 150 patients (72.0%). It's noteworthy that female patients were significantly older than their male counterparts.

**Table 1. Demographics of study patients with suspected cardiac amyloidosis**

| Total (n=150) | Female | Male | P value |
|---|---|---|---|
| n, % | 42 (28%) | 108 (72%) | |
| Age, y | 73.5±10.2 | 70.6±11.7 | 0.01 |

## 3.2 Diagnostic tests used in patients with suspected cardiac amylodosis

### 3.2.1 Myocardial biopsy

Myocardial biopsy was performed in only a small subset of patients, specifically, n = 16 (10.7%). It's noteworthy that the majority of these cases yielded positive results for cardiac amyloidosis, with a total of n = 14 out of 16 (87,5%). Among the patients with histopathologically confirmed cardiac amyloidosis, 7 were immunohistochemically diagnosed with the ATTR type, while the remaining patients had other types of cardiac amyloidosis, primarily AL.

### 3.2.2 Cardiac MRI

Cardiac MRI imaging was performed on a subset of 77 patients, representing 51% of the total study cohort. Within this group, positive cardiac amyloidosis findings were

identified in 44 patients, making up 57% of those who underwent cardiac MRI. The summarized data for the two diagnostic assessments mentioned above can be found in Table 2.

**Table 2. Summary of myocardial biopsy and cardiac MRI**

| Myocardial biopsy | n (%) | Results | n |
|---|---|---|---|
| Yes | 16 (10,7%) | Positive | 14 (87,5%) |
| | | Negative | 2 (12,5%) |
| N0 | 134 (89.3%) | - | - |
| Total | 150 | - | 16 |

| Cardiac MRI | n (%) | Results | n |
|---|---|---|---|
| Yes | 77 (51,3%) | Positive | 44 (57%) |
| | | Negative | 33 (43%) |
| N0 | 73 (48,7%) | - | - |
| Total | 150 | - | 77 |

### 3.2.3 Amyloid scintigraphy with $^{99m}$Tc-PYP

Myocardial scintigraphy with $^{99m}$ Tc-PYP involved two methods for assessing myocardial tracer uptake in the cohort of 150 participants:

a) Semi-quantitative visual grading of myocardial $^{99m}$Tc-PYP uptake based on the Perugini score (0 = absent, 1 = mild, 2 = moderate, 3 = high).

b) Quantification of cardiac $^{99m}$Tc-PYP uptake using the heart-to-contralateral lung (H/CL) ratio, calculated by delineating a region of interest (ROI) over the heart in the standard manner.

Regarding the visual grading of myocardial $^{99m}$Tc-PYP uptake, Figure 9 illustrates the frequency and percentage distribution of Perugini scores among the study

participants. Scintigraphy findings reveal myocardial uptake with scores ranging from 1 to 3 in 133 patients, representing 88.7% of the total cohort, indicative of $^{99m}$Tc-PYP accumulation. In contrast, 17 patients (11.3%) received a score of 0.

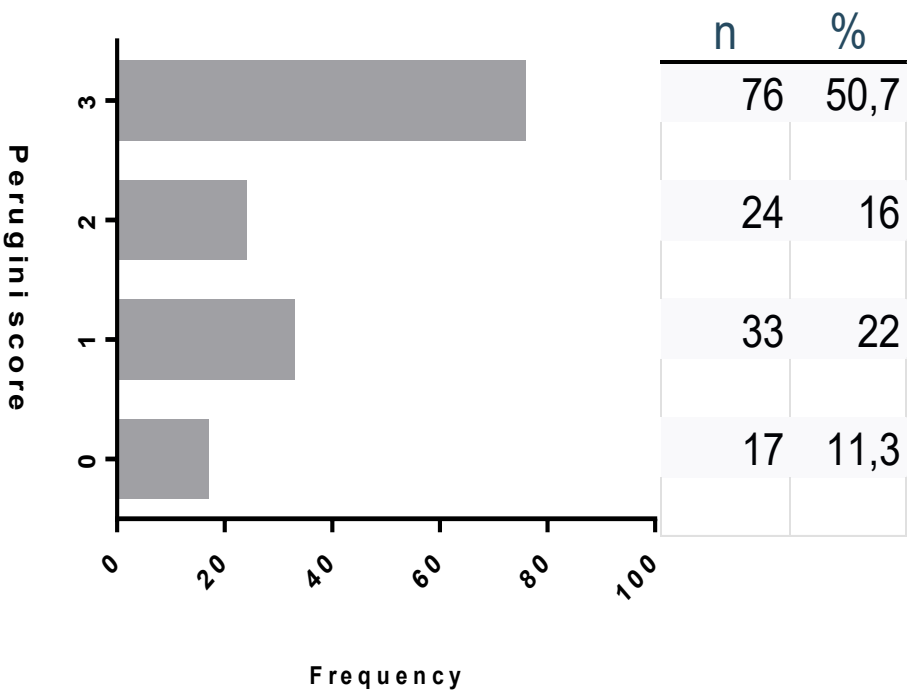


**Figure 9. The frequency and percentage distribution of Perugini scores among the patient with suspected cardiac amyloidosis**

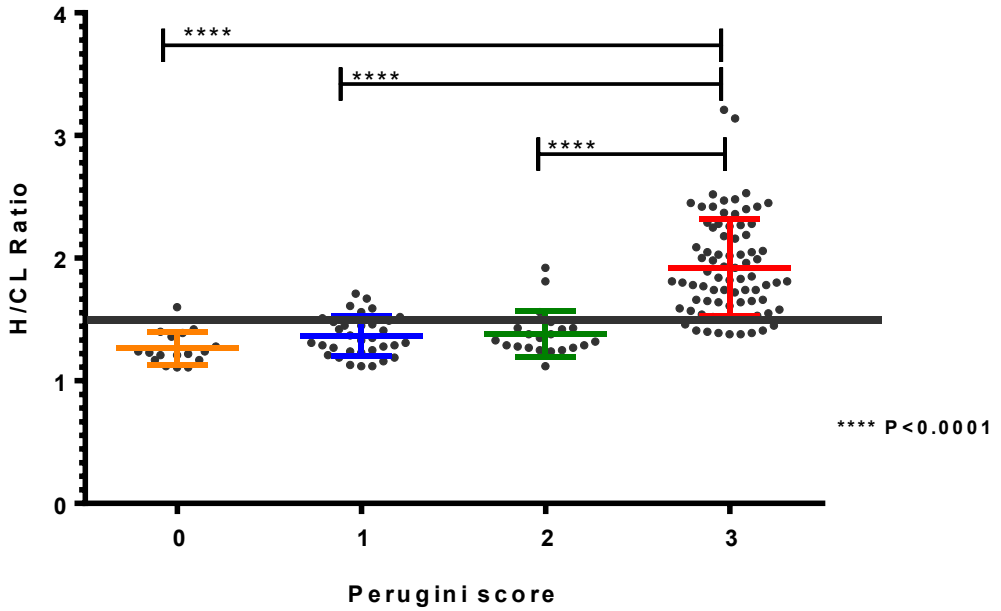


| | Score 0 | Score 1 | Score 2 | Score 3 |
|---|---|---|---|---|
| **H/CL ratio 1-1.5** | 16 (10,7%) | 26 (17,2%) | 18 (12%) | 10 (6,7%) |
| **H/CL ratio >1.5** | 1 (0,7%) | 7 (4,7%) | 4 (2,7%) | 68 (45,3%) |

**Figure 10. Heart-to-contralateral lung ratio (H/CL) compared to Perugini score in the patient with suspected cardiac amyloidosis**

The determined heart-to-contralateral lung ratio (H/CL), obtained by delineating a region of interest (ROI) over the heart using a standardized method, was categorized into two groups: values between 1 and 1.5, constituting 70 patients (46.6%), and those greater than 1.5, accounting for 80 patients (53.4%). These data are presented based on their distribution in Perugini score groups in Figure 10 above.

### 3.3 Sensitivity and specificity of myocardial $^{99m}$Tc-PYP uptake based on Perugini score and H/CL ratio

In this section of the study, we compared the results of myocardial $^{99m}$Tc-PYP uptake based on the Perugini score and the H/CL ratio with the results of myocardial biopsy and cardiac MRI, which are considered the standard methods for diagnosing myocardial amyloidosis. We employed cross-tabulation methods for this comparison.

The sensitivity and specificity analysis for both study methods applied to patients diagnosed with myocardial amyloidosis through myocardial biopsy demonstrated remarkably high sensitivity. Furthermore, the sensitivity and specificity analysis for both study methods in patients diagnosed with myocardial amyloidosis through cardiac MRI also showed strong performance. Upon examining the results, we found that the Perugini scoring method exhibited a sensitivity of 92% and a specificity of 33%. In simple terms, a Perugini score of 0 indicates no disease, while scores of 1, 2, and 3 represent mild, moderate, and severe amyloidosis. Importantly, the Perugini score correctly identified 92% of patients with confirmed myocardial amyloidosis based on biopsy results.

On the other hand, the H/CL ratio demonstrated a specificity of 67% and a sensitivity of 54%. Its high specificity means that when the H/CL ratio is less than 1.5, it almost always correctly identifies patients without the disease, resulting in a very low rate of false positives.

When comparing the results obtained from cardiac MRI, we found a high sensitivity of 91% and specificity of 15%, respectively for the Perugini score, and 64% and 64%, respectively for the H/CL ratio. This means that these diagnostic methods are comparable to myocardial biopsy, considered the gold standard. For a more detailed overview of these results, please refer to Tables 3-6.

| | Disease present | Disease absent |
|---|---|---|
| **Test positive** | a (TP) | b (FP) |
| **Test negative** | c (FN)<br>***Sensitivity: a / a+c*** | d (TN)<br>***Specificity: d / b+d*** |
| TP: True positive, FP: Fals positive, FN: False negative, TN: True negative | | |

**Table 3. Crosstabulation of Perugini score and myocardial biopsy results**

| | | Myocardial biopsy results (Gold standard) | | |
|---|---|---|---|---|
| | | **amyloidosis** | **non-amyloidosis** | Total |
| **Preugini-score (0 v.s 1/2/3)** | mild/moderat/strong cardiac uptake (1/2/3) | **12 *** | **2** | **14** |
| | no cardiac uptake (0) | **1** | **1 **** | **2** |
| | Total | **13** | **3** | **16** |
| | ***Sensitivity: 92% (12/13)** **Specificity: 33% (1/3)** | | | |

**Table 4. Crosstabulation of H/CL ratio and myocardial biopsy results**

| | | Myocardial biopsy results (Gold standard) | | |
|---|---|---|---|---|
| | | **amyloidosis** | **non-amyloidosis** | Total |
| **H/CL ratio** | H/CL ratio > 1.5 | **7*** | **1** | **8** |
| | H/CL ratio <=1.5 | **6** | **2 **** | **8** |
| | Total | **13** | **3** | **16** |
| | ***Sensitivity: 54% (7/13)** **Specificity: 67% (2/3)** | | | |

**Table 5. Crosstabulation of Perugini score (0 vs.1|2|3) vs. cardiac MRI results**

| | | Cardiac MRI | | |
|---|---|---|---|---|
| | | amyloidosis | non-amyloidosis | Total |
| Preugini-score (0 v.s 1/2/3) | mild/moderat/strong cardiac uptake (1/2/3) | **40 *** | **28** | **68** |
| | no cardiac uptake (0) | **4** | **5 **** | **9** |
| | Total | **44** | **33** | **44** |
| | ***Sensitivity: 91% (40/44) **Specificity: 15% (5/33)** | | | |

**Table 6. Crosstabulation of H/CL ratio and cardiac MRI results**

| | | Cardiac MRI | | |
|---|---|---|---|---|
| | | amyloidosis | non-amyloidosis | Total |
| H/CL ratio | H/CL ratio > 1.5 | **28*** | **12** | **39** |
| | H/CL ratio ≤1.5 | **16** | **21 **** | **38** |
| | Total | **44** | **33** | **77** |
| | ***Sensitivity: 64% (28/44) **Specificity: 64% (21/33)** | | | |

### 3.4 The frequency of death in relation to the type of diagnostic methods

The following tables illustrate the frequency of death within the study groups. The results show that seventeen patients died due to amyloidosis. As depicted in Table 7, sixteen out of the seventeen deaths from amyloidosis had mild to strong uptake, as indicated by a Perugini score of 1/2/3 during the examination. Only one death case from this group showed no uptake. This underscores the high sensitivity of the Perugini score in detecting amyloidosis in patients.

Similarly, when evaluating the death group based on H/CL examination, it is evident that more than 65% of the deceased cases (11 cases) had an H/CL ratio over 1.5,

which is indicative of amyloidosis. In contrast, 6 cases had an H/CL ratio lower than 1.5, signifying the absence of amyloidosis. These results are presented in Table 8.

**Table 7. Crosstabulation of death and Perugini score results (0 vs.1/2/3)**

| | | Perugini-score (0 vs. 1\|2 3) | | |
|---|---|---|---|---|
| | | mild/moderat/strong cardiac uptake | No cardiac uptake | Total |
| **Death** | no | 117 | 16 | 133 |
| | yes | 16 | 1 | 17 |
| **Toral** | | 133 | 17 | 150 |

**Table 8. Crosstabulation of death and H/CL ratio results**

| | | H/CL ratio | | |
|---|---|---|---|---|
| | | > 1.5 | <=1.5 | Total |
| **Death** | no | 69 | 64 | 133 |
| | yes | 11 | 6 | 17 |
| **Toral** | | 80 | 70 | 150 |

### 3.5 Follow-up function within alive patients with suspected cardiac amyloidosis

In order to be able to analyze the average survival time of the patients a Kaplan-Meier curve was created. For this purpose, the recorded follow-up up to 11/2022 was correlated with the event of death. The median follow-up is 9 months (range 0.3 - 49 months). The median survival in patients with mild, moderate, and strong cardiac uptake (Perugini score 1-3) was 9 months compared to 7 months in patients with no cardiac uptake (Perugini score 0). In patients with a H/CL ratio > 1.5 the median survival was 12 mo compared to 7 mo in patients with H/CL ratio ≤ 1.5. Among the 16 patients with performed myocardial biopsy the median survival was 5 mo in patients with histologically proven cardiac amyloidosis compared to 6 mo in patients without

CA. Among the 77 patients with cardiac MRI the median survival was 10 mo in patients with CA compared to 12 mo in patients without CA. This data is presented in Table 9.

**Table 9. Mean and median survival in months in patients with suspect cardiac amyloidosis**

| Perugini score group (n=150) | Mean mo | Median mo | No of pts. |
|---|---|---|---|
| mild/moderat/strong cardic uptake | 14,1 | 9 | 133 |
| No uptake | 11,9 | 7 | 17 |
| Total | 13 | 8 | 150 |

| H/CL ratio group (n=150) | Mean mo | Median mo | No of pts. |
|---|---|---|---|
| > 1.5 | 15,7 | 12 | 80 |
| ≤1.5 | 11,7 | 7 | 70 |
| Total | 13,7 | 9,5 | 150 |

| Myocardial biopsy group (n=16) | Mean | Median | No of pts. |
|---|---|---|---|
| Cardiac amyloidosis | 11,9 | 5 | 13 |
| non-amyloidosis | 8 | 6 | 3 |
| Total | 10 | 5,5 | 16 |

| Cardiac MRI group (n=77) | Mean mo | Median mo | No of pts. |
|---|---|---|---|
| Cardiac amyloidosis | 15 | 10 | 44 |
| non-amyloidosis | 12,6 | 12 | 33 |
| Total | 13,8 | 11 | 97 |

The following Kaplan-Meier curves illustrate the survival function based on various diagnostic methods in this study patient population. The Kaplan-Meier curves below show how each diagnostic approach correlates with patient survival. Seventeen patients died in the course of the follow-up. For the 133 patients who did not die, the follow-up ended with the last system note on medical care. These test subjects are censored in the Kaplan-Meier curve shown. We conducted statistical analysis using the log-rank (Mantel-Cox) test. The results of our analysis revealed the following:

The log-rank test for trend showed no significant difference in survival among the various Perugini score groups (p= 0.53) (Figure 11).

Similarly, there was no notable difference in survival between patients classified into two groups based on the H/CL ratio: those with a ratio of 1-1.5 and those with a ratio greater than 1.5 (p= 0.45) (Figure 12).

There was no significant difference in survival (p= 0.57) between patients with confirmed CA in myocardial biopsy and patients without CA (Figure 13).

Furthermore, the analysis of the cardiac MRI groups also indicated non-significant results (p= 0.9) (Figure 14).

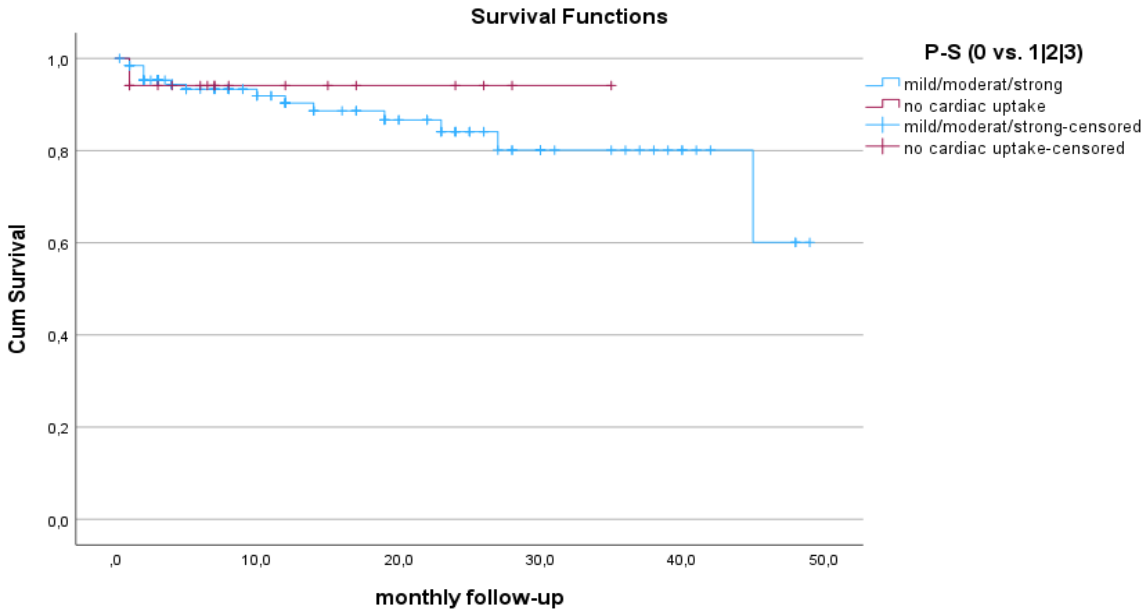


**Figure 11. The survival function based on Perugini score in patients with suspected cardiac amyloidosis**

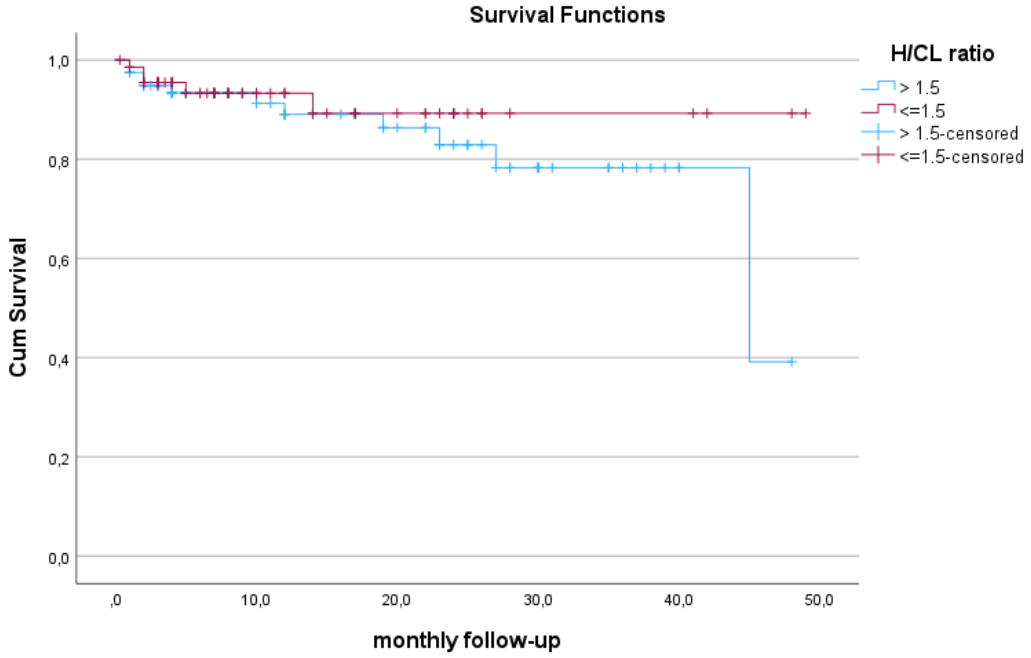


**Figure 12. The survival function based on H/CL ratio in patients with suspected cardiac amyloidosis**

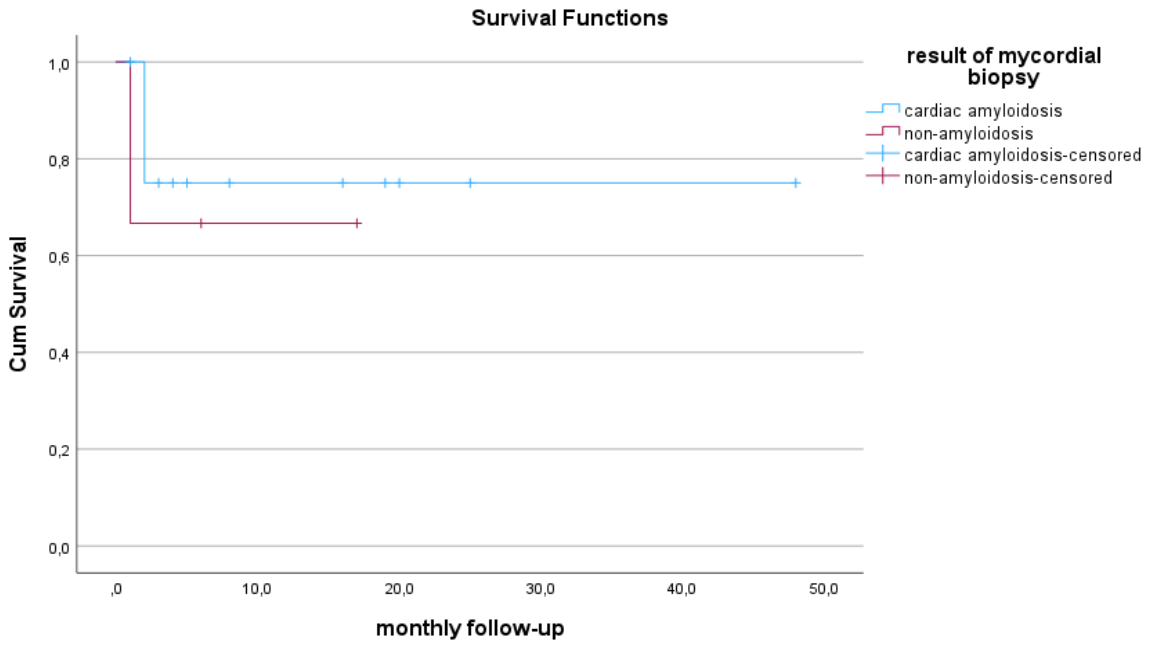


**Figure 13. The survival function based on myocardial biopsy in patients with suspected cardiac amyloidosis**

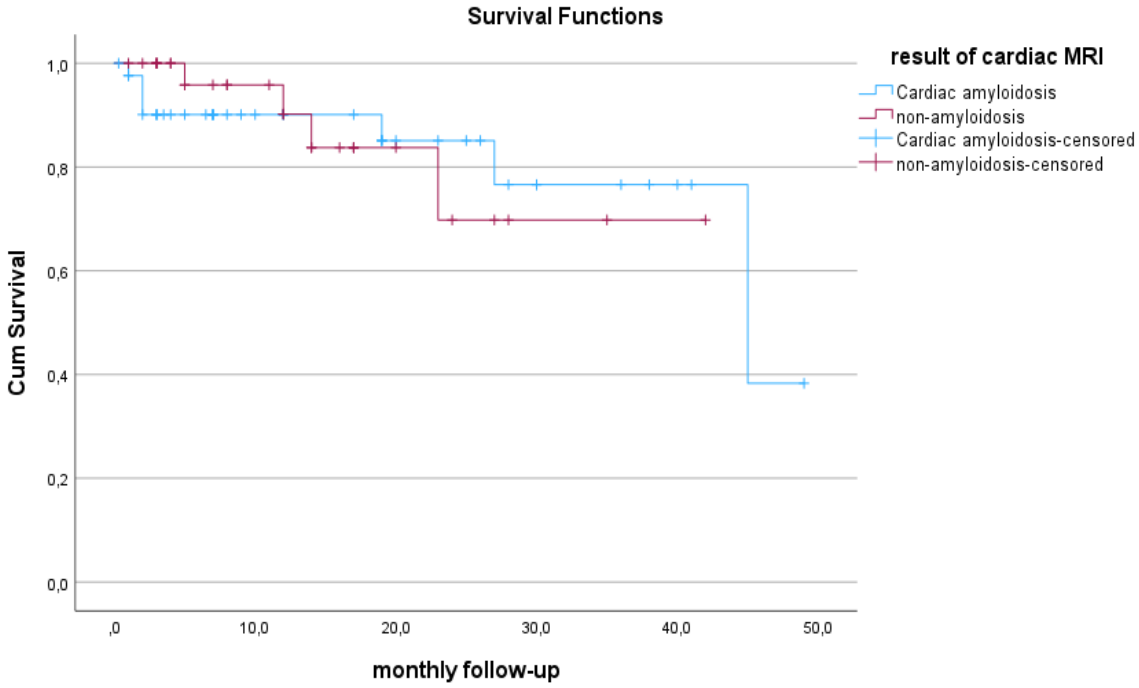


**Figure 14. The survival function based on cardiac MRI in patients with suspected cardiac amyloidosis**

### 3.6 The relationship between patient age and Perugini scoring in cardiac amyloidosis

Our study's data revealed a significant correlation between patient age and Perugini score in cardiac amyloidosis. We observed that patients with a Perugini score of 3 (mean 77.2 years) are notably ($p < 0.0001$) older than those with scores of 2 (mean 65.2 years) and 1 (mean 62.6 years). This finding is depicted in Figure 15 below.

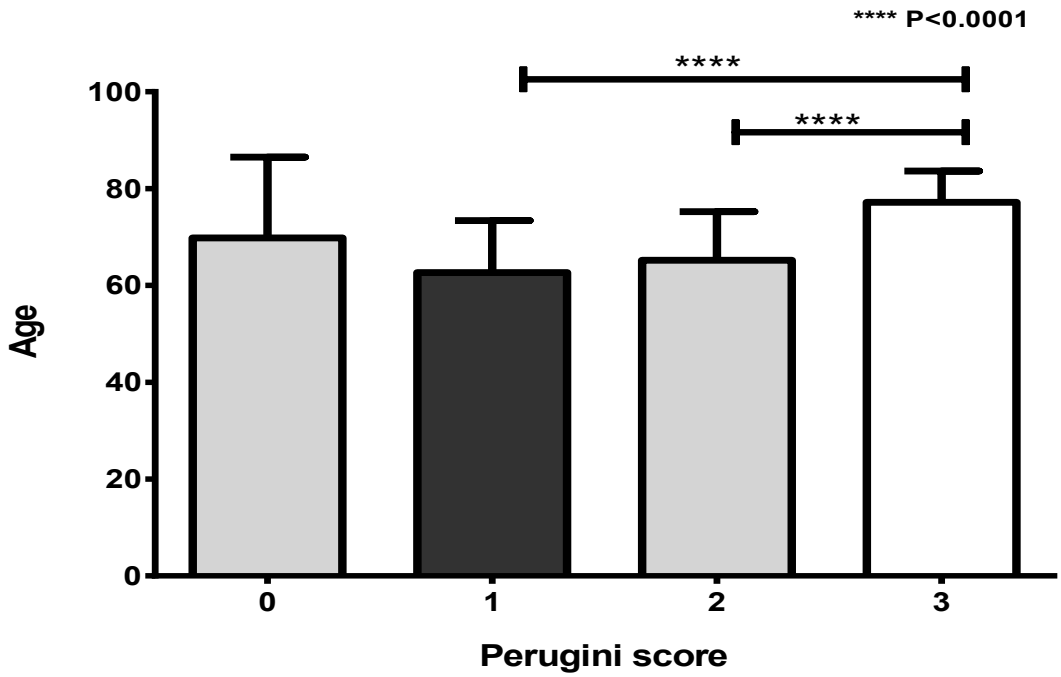


**Figure 15. Comparison of Perugini score and age in patients with suspected cardiac amyloidosis**

# 4 Discussion

## 4.1 Accuracy of the Perugini grading and H/CL ratio using $^{99m}$Tc-PYP amyloid scintigraphy in cardiac amyloidosis

The aim of the present study was to evaluate the diagnostic and prognostic value of amyloid scintigraphy with $^{99m}$Tc-PYP. We have assessed both qualitative and quantitative diagnostic methods. The qualitative method involves utilizing the Perugini score for visual assessment, while the quantitative method relies on determining the H/CL ratio. We compared the performance of these diagnostic methods with the findings derived from potential myocardial biopsies, which serve as the gold standard, and heart MRI scans, a frequently employed diagnostic tool. By conducting this evaluation in a real-world clinical setting, we aimed to contribute valuable insights that can improve the early detection and management of cardiac amyloidosis.

Our study demonstrated myocardial uptake in 133 patients (88.7% with a Perugini score of 1-3) compared to 17 patients (11.3% with a Perugini score of 0). When examining the same group of patients using the H/CL ratio, a remarkable observation was made. In patients categorized with an H/CL ratio > 1.5, there was low dispersion in the data. Furthermore, over 86% of these patients were classified as Perugini score 3, which suggests a high level of diagnostic accuracy for Perugini scoring. In groups with H/CL ratios of ≤1.5, it's noteworthy that the lowest value corresponds to a Perugini score of 3, providing additional confirmation of the diagnosis's accuracy.

In this study, we have demonstrated that the qualitative Perugini score exhibits very high sensitivity, reaching 92% and 91%, and specificity of 33% and 15% in diagnosing cardiac amyloidosis using myocardial biopsy and cardiac MRI as gold standard, respectively. On the other hand, our results indicate that, when compared to myocardial biopsy and cardiac MRI, the quantitative H/CL ratio displays a good specificity of 67% and 64% and sensitivity of 54% and 64% respectively. Thus, our results are comparable with the results of other studies using $^{99m}$Tc-PYP regarding sensitivity.

In 2012, Yamamoto Y et al. evaluated the utility of $^{99m}$Tc-PYP SPECT using the PYP score as quantitative method in 13 subjects with heart failure due to amyloid and 37 subjects with heart failure attributed to non-amyloid causes [24]. The investigators defined the PYP score as the ratio of myocardial mean counts to ventricular cavity

mean counts and achieved a sensitivity of 84.6% and a specificity of 94.5% for distinguishing cardiac amyloidosis from non-amyloid causes of heart failure [24]. In simpler terms, their method is highly sensitive in correctly identifying cases of cardiac amyloidosis and has a strong ability to rule out other potential causes of heart failure.

Bokhari S et al. conducted a study using $^{99m}$Tc-PYP and obtained significant practical results through quantitative analysis of myocardial uptake [23]. Their prospective cohort study included 45 patients with biopsy-proven AL or ATTR amyloidosis, in which they achieved a sensitivity of 97% and specificity of 100% for $^{99m}$Tc-PYP single-photon emission computed tomography (SPECT) in differentiating between light-chain cardiac amyloidosis and transthyretin-related amyloidosis [23]. Thus, the $^{99m}$Tc -PYP SPECT method demonstrated an exceptionally high degree of accuracy in distinguishing between AL and ATTR cardiac amyloidosis [23]. This finding is particularly promising for the diagnosis and classification of these conditions.

However, it's important to note that Hutt DF et al. reported that $^{99m}$Tc-DPD scintigraphy is highly sensitive for identifying cardiac ATTR amyloidosis [25]. Still, they found that stratification by Perugini grade of positivity at diagnosis does not carry prognostic significance. In essence, while $^{99m}$Tc-DPD scintigraphy is excellent for detecting ATTR amyloidosis, the degree of positivity at diagnosis does not appear to correlate with the prognosis [25].

It should be noted, as described by Gillmore JD et al., that in patients with cardiac uptake of $^{99m}$Tc-PYP (Perugini score 1,2,3), if the results of serum and urine immunofixation and free light chain assay are negative, there is no need to confirm the histology and type of amyloidosis. This supports the diagnosis of cardiac ATTR amyloidosis [27]. In the next stage, the TTR genotype test can be used to differentiate between variant ATTR amyloidosis and wild-type ATTR amyloidosis [27].

Poterucha, TJ and colleagues showed that SPECT can improve specificity compared to planar imaging alone using $^{99m}$Tc-PYP scintigraphy with imaging one hour after injection in patients with ATTR-CA [49]. When compared to SPECT imaging as a reference standard, planar imaging produced false positive results in 16 out of 25 (64%) grade 2 scans. These findings provide valuable insights into the diagnostic

accuracy and potential limitations of these imaging methods in assessing ATTR-CA [49].

## 4.2 The prognostic value of Perugini grading and H/CL ratio in $^{99m}$Tc-PYP scintigraphy in cardiac amyloidosis

The predictive value of Perugini grading and the heart-to-contralateral lung (H/CL) ratio in $^{99m}$Tc-PYP scintigraphy is crucial for the management of cardiac amyloidosis. These assessment methods not only aid in the diagnosis and characterization of cardiac amyloidosis but also provide valuable prognostic insights.

In our study, we observed no significant differences in survival for Perugini score, H/CL ratio, cardiac MRI, and myocardial biopsy among the different groups or categories. For cardiac amyloidosis patients with mild, moderate, and strong $^{99m}$Tc-PYP uptake, as indicated by a Perugini score of 1-3, the median survival time was 9 months. In contrast, non-cardiac amyloidosis patients with no uptake, corresponding to a Perugini score of 0, had a median survival of 7 months. Similarly, patients diagnosed with an H/CL ratio greater than 1.5 had a median survival of 12 months, while those with a ratio lower than 1.5 had a median survival time of 7 months. These findings underscore the variations in median survival among different diagnostic methods, with no significant differences observed. One possible explanation for this phenomenon could be that amyloidosis patients had longer periods of ongoing monitoring and follow-up compared to non-amyloidosis patients. The longer survival for amyloidosis patients may be attributed to the complexity and management of the condition, necessitating continuous medical attention and assessment.

Furthermore, our data strongly support a clear association between patient age and Perugini score in cases of cardiac amyloidosis. Significantly, patients with a Perugini score of 3 are notably older ($p < 0.0001$) than those with scores of 2 and 1. These findings consistently highlight an older age at disease onset and a higher prevalence of severe cardiac involvement within this specific population.

Interestingly, our findings align with those of Hutt DF et al., who examined survival from the time of $^{99m}$Tc-DPD scintigraphy in 602 patients with ATTR amyloidosis, including 377 with wild-type ATTR (ATTRwt) and 225 with mutant ATTR (ATTRm)

amyloidosis [50]. They stratified patients according to Perugini grade (0-3) on the $^{99m}$Tc-DPD scan and assessed the prognostic significance of additional patient and disease-related factors at baseline. In the overall cohort, they observed that a Perugini grade 0 on the $^{99m}$Tc-DPD scan was consistently associated with the absence of cardiac amyloidosis according to consensus criteria, as well as significantly better patient survival compared to Perugini grades 1, 2, or 3 on the $^{99m}$Tc-DPD scan ($P < 0.005$). However, there were no significant differences in survival between patients with grade 1, grade 2, or grade 3 $^{99m}$Tc-DPD scans in ATTRwt, V122I-associated ATTRm, or T60A–associated ATTRm amyloidosis. They concluded that $^{99m}$Tc-DPD scintigraphy is highly sensitive for identifying cardiac ATTR amyloid but stratification by Perugini grade at diagnosis does not carry prognostic significance [50].

Our findings are in line with those of Rapezzi C et al. showing that the disease typically manifests relatively late, with an average age of of onset of around 73.5 years [20]. The authors observed a notable age difference between patients with a Perugini score of 3 and those with scores of 2 and 1 [20].

Our study has several limitations. Firstly, only 16 patients had myocardial biopsy being the gold standard for the diagnosis of CA. Secondly, only 77/150 patients underwent cardiac MRI, also used as the reference method. Thirdly, in only 48/150 patients SPECT/CT was performed. Therefore, in the present study only planar images were evaluated. If the SPECT/CT images had also been taken into account, the specificity would probably have been improved by reducing the number of false positive cases. Possible future studies of amyloid scintigraphy with $^{99m}$Tc-PYP should include only patients who have performed SPECT/CT of the heart. Using SPECT/CT could differentiate blood pool from myocardial uptake.

### 4.3 Conclusion

In this retrospective study with 150 patients with suspected cardiac amyloidosis, $^{99m}$Tc-PYP scintigraphy revealed a high sensitivity with 92% but low specificity with 33% for visual diagnosis of cardiac amyloidosis (Perugini score) using myocardial biopsy as reference method. Using cardiac MRI as reference method the Perugini score exhibited a high sensitivity of 91% and a very low specificity of 15%.

In contrast, the quantitative H/CL ratio demonstrated a good specificity of 67% and 64% and moderate sensitivity of 54% and 64% using myocardial biopsy and cardiac MRI as reference methods, respectively.

Using SPECT may have improved specificity. However, in the present study only planar images were evaluated because only 48 patients (32%) had SPECT/CT imaging of the heart. It should be noted that a Perugini score of 3 does not automatically mean ATTR-CA, unless AL amyloidosis has been ruled out in the serum or by urine immunofixation and free light chain assay beforehand. Notably, our study did not reveal any significant differences in survival time between the groups tested with the Perugini score and H/CL ratio.

These findings emphasize the importance of extended monitoring and care for individuals with cardiac amyloidosis, as the condition requires ongoing attention and management.

However, in our study, patients with CA and, therefore, a higher Perugini score, and H/CL ratio demonstrated a slightly higher median survival compared to patients without CA. From this it can be concluded that stratification according to Perugini score and H/CL ratio has no prognostic value in patients with suspected cardiac amyloidosis.

In summary, our findings highlight the potential of $^{99m}$Tc-PYP scintigraphy and the H/CL ratio as effective and sensitive diagnostic tools that may offer advantages over the conventional myocardial biopsy approach. These methods provide valuable insights into the diagnosis and management of cardiac amyloidosis, offering the possibility of earlier detection and improved patient care.

# 5 References


1. Lachmann HJ, Hawkins PN: Systemic amyloidosis. *Curr Opin Pharmacol* 2006, 6(2):214-220.

2. Pinney JH, Hawkins PN: Amyloidosis. *Ann Clin Biochem* 2012, 49(Pt 3):229-241.

3. Muchtar E, Gertz MA, Kumar SK, Lacy MQ, Dingli D, Buadi FK, Grogan M, Hayman SR, Kapoor P, Leung N *et al*: Improved outcomes for newly diagnosed AL amyloidosis between 2000 and 2014: cracking the glass ceiling of early death. *Blood* 2017, 129(15):2111-2119.

4. Patel KS, Hawkins PN: Cardiac amyloidosis: where are we today? *J Intern Med* 2015, 278(2):126-144.

5. Carr AS, Pelayo-Negro AL, Jaunmuktane Z, Scalco RS, Hutt D, Evans MR, Heally E, Brandner S, Holton J, Blake J *et al*: Transthyretin V122I amyloidosis with clinical and histological evidence of amyloid neuropathy and myopathy. *Neuromuscul Disord* 2015, 25(6):511-515.

6. Rapezzi C, Quarta CC, Obici L, Perfetto F, Longhi S, Salvi F, Biagini E, Lorenzini M, Grigioni F, Leone O *et al*: Disease profile and differential diagnosis of hereditary transthyretin-related amyloidosis with exclusively cardiac phenotype: an Italian perspective. *Eur Heart J* 2013, 34(7):520-528.

7. Banypersad SM, Moon JC, Whelan C, Hawkins PN, Wechalekar AD: Updates in cardiac amyloidosis: a review. *J Am Heart Assoc* 2012, 1(2):e000364.

8. Martinez-Naharro A, Hawkins PN, Fontana M: Cardiac amyloidosis. *Clin Med (Lond)* 2018, 18(Suppl 2):s30-s35.

9. Adam RD, Coriu D, Jercan A, Badelita S, Popescu BA, Damy T, Jurcut R: Progress and challenges in the treatment of cardiac amyloidosis: a review of the literature. *ESC Heart Fail* 2021, 8(4):2380-2396.

10. Baker KR, Rice L: The amyloidoses: clinical features, diagnosis and treatment. *Methodist Debakey Cardiovasc J* 2012, 8(3):3-7.

11. Ton VK, Mukherjee M, Judge DP: Transthyretin cardiac amyloidosis: pathogenesis, treatments, and emerging role in heart failure with preserved ejection fraction. *Clin Med Insights Cardiol* 2014, 8(Suppl 1):39-44.

12. Bhuiyan T, Helmke S, Patel AR, Ruberg FL, Packman J, Cheung K, Grogan D, Maurer MS: Pressure-volume relationships in patients with transthyretin (ATTR) cardiac amyloidosis secondary to V122I mutations and wild-type transthyretin: Transthyretin Cardiac Amyloid Study (TRACS). *Circ Heart Fail* 2011, 4(2):121-128.

13. Maurer MS: Non-invasive Identification of ATTRwt Cardiac Amyloid: The Re-emergence of Nuclear Cardiology. *Am J Med* 2015, 128(12):1275-1280.

14. Siddiqi OK, Ruberg FL: Cardiac amyloidosis: An update on pathophysiology, diagnosis, and treatment. *Trends Cardiovasc Med* 2018, 28(1):10-21.

15. Gilstrap LG, Dominici F, Wang Y, El-Sady MS, Singh A, Di Carli MF, Falk RH, Dorbala S: Epidemiology of Cardiac Amyloidosis-Associated Heart Failure Hospitalizations Among Fee-for-Service Medicare Beneficiaries in the United States. *Circ Heart Fail* 2019, 12(6):e005407.

16. Mejia Baranda J, Ljungberg J, Wixner J, Anan I, Oskarsson V: Epidemiology of hereditary transthyretin amyloidosis in the northernmost region of Sweden: a retrospective cohort study. *Amyloid* 2022, 29(2):120-127.

17. Pinney JH, Whelan CJ, Petrie A, Dungu J, Banypersad SM, Sattianayagam P, Wechalekar A, Gibbs SD, Venner CP, Wassef N *et al*: Senile systemic amyloidosis: clinical features at presentation and outcome. *J Am Heart Assoc* 2013, 2(2):e000098.

18. Kittleson MM, Maurer MS, Ambardekar AV, Bullock-Palmer RP, Chang PP, Eisen HJ, Nair AP, Nativi-Nicolau J, Ruberg FL, American Heart Association Heart F *et al*: Cardiac Amyloidosis: Evolving Diagnosis and Management: A

Scientific Statement From the American Heart Association. *Circulation* 2020, 142(1):e7-e22.

19. Kumar S, Dispenzieri A, Katzmann JA, Larson DR, Colby CL, Lacy MQ, Hayman SR, Buadi FK, Leung N, Zeldenrust SR *et al*: Serum immunoglobulin free light-chain measurement in primary amyloidosis: prognostic value and correlations with clinical features. *Blood* 2010, 116(24):5126-5129.

20. Rapezzi C, Merlini G, Quarta CC, Riva L, Longhi S, Leone O, Salvi F, Ciliberti P, Pastorelli F, Biagini E *et al*: Systemic cardiac amyloidoses: disease profiles and clinical courses of the 3 main types. *Circulation* 2009, 120(13):1203-1212.

21. Sado DM, Flett AS, Banypersad SM, White SK, Maestrini V, Quarta G, Lachmann RH, Murphy E, Mehta A, Hughes DA *et al*: Cardiovascular magnetic resonance measurement of myocardial extracellular volume in health and disease. *Heart* 2012, 98(19):1436-1441.

22. Rapezzi C, Quarta CC, Guidalotti PL, Pettinato C, Fanti S, Leone O, Ferlini A, Longhi S, Lorenzini M, Reggiani LB *et al*: Role of (99m)Tc-DPD scintigraphy in diagnosis and prognosis of hereditary transthyretin-related cardiac amyloidosis. *JACC Cardiovasc Imaging* 2011, 4(6):659-670.

23. Bokhari S, Castano A, Pozniakoff T, Deslisle S, Latif F, Maurer MS: (99m)Tc-pyrophosphate scintigraphy for differentiating light-chain cardiac amyloidosis from the transthyretin-related familial and senile cardiac amyloidoses. *Circ Cardiovasc Imaging* 2013, 6(2):195-201.

24. Yamamoto Y, Onoguchi M, Haramoto M, Kodani N, Komatsu A, Kitagaki H, Tanabe K: Novel method for quantitative evaluation of cardiac amyloidosis using (201)TlCl and (99m)Tc-PYP SPECT. *Ann Nucl Med* 2012, 26(8):634-643.

25. Hutt DF, Quigley AM, Page J, Hall ML, Burniston M, Gopaul D, Lane T, Whelan CJ, Lachmann HJ, Gillmore JD *et al*: Utility and limitations of 3,3-diphosphono-1,2-propanodicarboxylic acid scintigraphy in systemic amyloidosis. *Eur Heart J Cardiovasc Imaging* 2014, 15(11):1289-1298.

26. Perugini E, Guidalotti PL, Salvi F, Cooke RM, Pettinato C, Riva L, Leone O, Farsad M, Ciliberti P, Bacchi-Reggiani L *et al*: Noninvasive etiologic diagnosis of cardiac amyloidosis using 99mTc-3,3-diphosphono-1,2-propanodicarboxylic acid scintigraphy. *J Am Coll Cardiol* 2005, 46(6):1076-1084.

27. Gillmore JD, Maurer MS, Falk RH, Merlini G, Damy T, Dispenzieri A, Wechalekar AD, Berk JL, Quarta CC, Grogan M *et al*: Nonbiopsy Diagnosis of Cardiac Transthyretin Amyloidosis. *Circulation* 2016, 133(24):2404-2412.

28. Cuddy S, Falk R, Dorbala S: Molecular Imaging of Cardiac Amyloidosis. *Current Cardiovascular Imaging Reports* 2018, 11(7):17.

29. Schaadt BK, Hendel HW, Gimsing P, Jonsson V, Pedersen H, Hesse B: 99mTc-aprotinin scintigraphy in amyloidosis. *J Nucl Med* 2003, 44(2):177-183.

30. Khaw BA, Narula J: Antibody imaging in the evaluation of cardiovascular diseases. *J Nucl Cardiol* 1994, 1(5 Pt 1):457-476.

31. Asghar O, Arumugam P, Armstrong I, Ray S, Schmitt M, Malik RA: Iodine-123 metaiodobenzylguanidine scintigraphy for the assessment of cardiac sympathetic innervation and the relationship with cardiac autonomic function in healthy adults using standardized methods. *Nucl Med Commun* 2017, 38(1):44-50.

32. Schindler TH, Sharma V, Imperiale A: (18)F-Florbetaben and PET/CT Holds Promise for the Identification and Differentiation Among Cardiac Amyloidosis Entities. *JACC Cardiovasc Imaging* 2021, 14(1):256-258.

33. Genovesi D, Vergaro G, Giorgetti A, Marzullo P, Scipioni M, Santarelli MF, Pucci A, Buda G, Volpi E, Emdin M: [18F]-Florbetaben PET/CT for Differential Diagnosis Among Cardiac Immunoglobulin Light Chain, Transthyretin Amyloidosis, and Mimicking Conditions. *JACC Cardiovasc Imaging* 2021, 14(1):246-255.

34. Castano A, Helmke S, Alvarez J, Delisle S, Maurer MS: Diflunisal for ATTR cardiac amyloidosis. *Congest Heart Fail* 2012, 18(6):315-319.

35. Stern LK, Patel J: Cardiac Amyloidosis Treatment. *Methodist Debakey Cardiovasc J* 2022, 18(2):59-72.

36. Verma B, Patel P: Tafamidis. In: *StatPearls.* edn. Treasure Island (FL); 2023.

37. Carvalho A, Rocha A, Lobato L: Liver transplantation in transthyretin amyloidosis: issues and challenges. *Liver Transpl* 2015, 21(3):282-292.

38. Patel KS, Hawkins PN, Whelan CJ, Gillmore JD: Life-saving implantable cardioverter defibrillator therapy in cardiac AL amyloidosis. *BMJ Case Rep* 2014, 2014.

39. Dey BR, Chung SS, Spitzer TR, Zheng H, Macgillivray TE, Seldin DC, McAfee S, Ballen K, Attar E, Wang T *et al*: Cardiac transplantation followed by dose-intensive melphalan and autologous stem-cell transplantation for light chain amyloidosis and heart failure. *Transplantation* 2010, 90(8):905-911.

40. Dispenzieri A, Gertz MA, Kyle RA, Lacy MQ, Burritt MF, Therneau TM, Greipp PR, Witzig TE, Lust JA, Rajkumar SV *et al*: Serum cardiac troponins and N-terminal pro-brain natriuretic peptide: a staging system for primary systemic amyloidosis. *J Clin Oncol* 2004, 22(18):3751-3757.

41. Aimo A, Merlo M, Porcari A, Georgiopoulos G, Pagura L, Vergaro G, Sinagra G, Emdin M, Rapezzi C: Redefining the epidemiology of cardiac amyloidosis. A systematic review and meta-analysis of screening studies. *Eur J Heart Fail* 2022, 24(12):2342-2351.

42. Shams P, Ahmed I: Cardiac Amyloidosis. In: *StatPearls.* edn. Treasure Island (FL); 2023.

43. Schicha H SO: Nuklearmedizin. Basiswissen und klinische Anwendung 7. Auflage edn. Stuttgart: Schattauer; 2013.

44. Shetty M: A cardiology fellow's take-home points from ASNC's Webinar: Cases in Tc 99m-PYP evaluation of ATTR cardiac amyloidosis - interpretation and reporting. *J Nucl Cardiol* 2021, 28(2):604-609.

45. Riefolo M, Conti M, Longhi S, Fabbrizio B, Leone O: Amyloidosis: What does pathology offer? The evolving field of tissue biopsy. *Front Cardiovasc Med* 2022, 9:1081098.

46. Musetti V, Greco F, Castiglione V, Aimo A, Palmieri C, Genovesi D, Giorgetti A, Emdin M, Vergaro G, McDonnell LA *et al*: Tissue Characterization in Cardiac Amyloidosis. *Biomedicines* 2022, 10(12).

47. Oda S, Kidoh M, Nagayama Y, Takashio S, Usuku H, Ueda M, Yamashita T, Ando Y, Tsujita K, Yamashita Y: Trends in Diagnostic Imaging of Cardiac Amyloidosis: Emerging Knowledge and Concepts. *Radiographics* 2020, 40(4):961-981.

48. Fontana M, Chung R, Hawkins PN, Moon JC: Cardiovascular magnetic resonance for amyloidosis. *Heart Fail Rev* 2015, 20(2):133-144.

49. Poterucha TJ, Elias P, Bokhari S, Einstein AJ, DeLuca A, Kinkhabwala M, Johnson LL, Flaherty KR, Saith SE, Griffin JM *et al*: Diagnosing Transthyretin Cardiac Amyloidosis by Technetium Tc 99m Pyrophosphate: A Test in Evolution. *JACC Cardiovasc Imaging* 2021, 14(6):1221-1231.

50. Hutt DF, Fontana M, Burniston M, Quigley AM, Petrie A, Ross JC, Page J, Martinez-Naharro A, Wechalekar AD, Lachmann HJ *et al*: Prognostic utility of the Perugini grading of 99mTc-DPD scintigraphy in transthyretin (ATTR) amyloidosis and its relationship with skeletal muscle and soft tissue amyloid. *Eur Heart J Cardiovasc Imaging* 2017, 18(12):1344-1350.